

Scattering function of semiflexible polymer chains under good solvent conditions

Hsiao-Ping Hsu^a, Wolfgang Paul^b, and Kurt Binder^a

^a*Institut für Physik, Johannes Gutenberg-Universität Mainz,
Staudinger Weg 7, D-55099 Mainz, Germany*

^b*Theoretische Physik, Martin Luther Universität
Halle-Wittenberg, von Seckendorffplatz 1,
06120 Halle, Germany*

Using the pruned-enriched Rosenbluth Monte Carlo algorithm, the scattering functions of semiflexible macromolecules in dilute solution under good solvent conditions are estimated both in $d = 2$ and $d = 3$ dimensions, considering also the effect of stretching forces. Using self-avoiding walks of up to $N = 25600$ steps on the square and simple cubic lattices, variable chain stiffness is modeled by introducing an energy penalty ϵ_b for chain bending; varying $q_b = \exp(-\epsilon_b/k_B T)$ from $q_b = 1$ (completely flexible chains) to $q_b = 0.005$, the persistence length can be varied over two orders of magnitude. For unstretched semiflexible chains we test the applicability of the Kratky-Porod worm-like chain model to describe the scattering function, and discuss methods for extracting persistence length estimates from scattering. While in $d = 2$ the direct crossover from rod-like chains to self-avoiding walks invalidates the Kratky-Porod description, it holds in $d = 3$ for stiff chains if the number of Kuhn segments n_K does not exceed a limiting value n_K^* (which depends on the persistence length). For stretched chains, the Pincus blob size enters as a further characteristic length scale. The anisotropy of the scattering is well described by the modified Debye function, if the actual observed chain extension $\langle X \rangle$ (end-to-end distance in the direction of the force) as well as the corresponding longitudinal and transverse linear dimensions $\langle X^2 \rangle - \langle X \rangle^2$, $\langle R_{g,\perp}^2 \rangle$ are used.

I. INTRODUCTION

Small angle (neutron) scattering from polymers in dilute solution is the method of choice to obtain a complete picture of the conformations of long flexible or semiflexible macromolecules, from the length scale of the monomeric units to the gyration radius of the chain molecules [1–4]. Classical experiments have shown that the gyration radius R_g of long flexible chains in dense melts (and also in dilute solution under Theta conditions) scales with chain length N according to the classical random walk picture [5–7], $R_g \propto N^{1/2}$, while in dilute solution under good solvent conditions flexible polymers form swollen coils [1–4, 8], $R_g \propto N^\nu$, with [9] $\nu \approx 0.588$ (in $d = 3$ dimensions) or $\nu = 3/4$ ($d = 2$). It was also shown that on intermediate length scales the dependence of the scattering intensity $S(q)$ on wave number q reflects the self-similar fractal structure of the polymer [8], $S(q) \propto q^{-1/\nu}$ (under good solvent conditions) or $S(q) \propto q^{-2}$ (Theta conditions or melts, respectively). Also the crossovers between these regimes when either the temperature distance from the Theta point or the concentration of the solution are varied have been investigated [4], and the length scales ruling these crossovers (i.e., diameter of “thermal blobs” or “concentration blobs”, respectively) have been identified [1–4].

The behavior gets more complicated, however, when chain stiffness plays a prominent role: only when chain stiffness is essentially due to chain thickness, i.e. when the effective persistence length ℓ_p scales proportional to the local chain diameter D the problem can still be reduced to a rescaled self-avoiding walk problem [10, 11]. However, when $\ell_p \gg D$, one finds (in $d = 3$) a double crossover, since then short chains behave like rigid

rods (i.e., $R_g \propto N$ as long as $R_g < \ell_p$), and then a crossover to Gaussian random-walk like coils occurs, while for $R_g \approx R_0$ (R_0 will be discussed below) a second crossover to swollen coils ($R_g \propto N^\nu$) starts. Also this behavior has been established in beautiful classical experiments [12], as well as in recent simulations [11, 13]. The standard model for semiflexible worm-like chains, the Kratky-Porod model [14], can only describe the first crossover (from rods to Gaussian coils) but fails to account for the second crossover to swollen coils, due to its complete neglect of excluded volume effects. It turns out that this second crossover still is incompletely understood: while in the early experiments [12] it was suggested that this crossover occurs for $n_K = n_K^*$ with $n_K^* = 50$ Kuhn segments, independent of the persistence length, a Flory-type argument [15, 16] suggests that the crossover occurs for a polymer radius $R_0 \propto \ell_p^2/D$ (corresponding to $n_K^* \propto (\ell_p/D)^2$), while the simulations rather find [13] $n_K^* \propto \ell_p^{1.5}$. Remember that a worm-like chain can be described as an equivalent freely jointed chain of n_K Kuhn segments of length $2\ell_p$ each [5, 6]. In view of an apparent conflict of the estimate [12] $n_K^* = 50$ with the Yamakawa-Stockmayer-Shimata theory [16–19] for worm-like chains the result $n_K^* = 50$ was considered as a very fundamental problem [20, 21]. However, Tsuboi et al [21] confirmed this estimate for another stiff polymer and concluded that the result $n_K^* = 50$ is compatible with the theory. We also note that in $d = 2$ there occurs a single crossover from rods to self-avoiding walks, any regime of Gaussian-like behavior is completely absent [13, 22]. We emphasize however, that the results of [11, 13, 15, 16] imply that a universal number n_K^* (independent of ℓ_p) up to which the Kratky-Porod model holds in $d = 3$ does not exist.

It then is interesting to ask how chain stiffness shows up on intermediate length scales, that can be probed via the scattering function $S(q)$. If one disregards excluded volume [1] and bases the treatment on the Kratky-Porod model, one can show [23] that the rod-like behavior at large q leads to a scattering law proportional to q^{-1} , i.e. (in $d = 3$ dimensions)

$$N\ell_b q S(q) = \pi + \frac{2}{3}(q\ell_p)^{-1}, \quad N \rightarrow \infty, \quad (1)$$

where we have assumed that the chain has a contour length $L = N\ell_b$, where ℓ_b is the bond length while the persistence length [6] is $\ell_p = (N/n_K)\ell_b/2$. While for Gaussian “phantom chains” (i.e., excluded volume interactions are completely neglected) the structure factor $S(q)$ is readily found [1–6] in terms of the Debye function, and the only length that enters is the gyration radius $\langle R_g^2 \rangle^{1/2}$, choosing a normalization where $S(q = 0) = 1$

$$S(q) = 2[\exp(-\zeta) - 1 + \zeta]/\zeta^2, \quad \zeta = q^2 \langle R_g^2 \rangle = q^2 N\ell_b^2/6, \quad (2)$$

for semiflexible polymers the calculation of $S(q)$ for chains with N finite is a formidable problem [24–39], even in the absence of excluded volume effects. However, including excluded volume effects in the description of scattering of semiflexible chains is even more an unsolved problem: existing phenomenological approaches require the adjustment of many empirical parameters [37]. It will be one of the tasks that will be addressed in the present paper, to investigate $S(q)$ for semiflexible chains numerically in the presence of excluded volume interactions between the effective monomers, varying ℓ_p over a wide range.

In recent years also the behavior of macromolecules under the influence of stretching forces has found enormous interest (e.g. [40–55]), in particular for the study of bio-macromolecules. Experimentally this can be realized e.g. by pulling at one end of a chain, that is anchored at a substrate with the other chain end, by the tip of an atomic force microscope [42, 46, 48, 49, 52, 55] but it is also conceivable to stretch polymers by the forces occurring when a polymer solution is exposed to strong

shear flow [56–58] or elongational flow [59]. Of course, it is not obvious that it will be possible to carry out scattering experiments on such stretched chains and measure the structure factor (which then is anisotropic and has two relevant parts $S_{||}(q_{||})$, $S_{\perp}(q_{\perp})$ since the direction of the scattering vector \vec{q} relative to the stretch direction, either parallel, $q_{||}$, or perpendicular, q_{\perp} , matters). But nevertheless a theoretical investigation of $S_{||}(q_{||})$, $S_{\perp}(q_{\perp})$ is worthwhile, because it gives detailed insight into the local structure of stretched chains, including also chains under cylindrical confinement [60–62] and this may help to understand problems such as transport of semiflexible polymers through porous materials, or channels in nanofluidic devices [60], etc. Thus we shall also investigate the structure factor of stretched semiflexible chains, extending previous work on flexible chains [40, 44].

The outline of our paper is as follows: in Sec. II, we give a summary of the theoretical background, and in Sec. III we define our model and briefly recall the simulation methodology. In Sec. IV we present our results for the structure factor $S(q)$ of semiflexible chains, for both $d = 2$ and $d = 3$ dimensions, in the absence of stretching forces. Sec. V describes the modifications of the structure factor due to stretching, while Sec. VI summarizes our conclusions. The calculation of the scattering function of random walk chains under constant pulling forces can be carried out analytically and is presented in an appendix.

II. THEORETICAL BACKGROUND

A. Definitions

We consider here the scattering from a single polymer chain, assuming that the chain can be described by a sequence of $N + 1$ (effective) monomers at positions \vec{r}_j , $j = 1, 2, \dots, N + 1$, so that we can define N bond vectors $\vec{a}_j = \vec{r}_{j+1} - \vec{r}_j$. In the absence of stretching forces, the structure factor $S(\vec{q})$ does not depend on the direction of the scattering vector \vec{q} , and can be defined as

$$\begin{aligned} S(q) &= \frac{1}{(N+1)^2} \left\langle \sum_{j=1}^{N+1} \sum_{k=1}^{N+1} \exp[i\vec{q} \cdot (\vec{r}_j - \vec{r}_k)] \right\rangle \\ &= \frac{1}{(N+1)^2} \left\{ \left\langle \left[\sum_{j=1}^{N+1} \sin(\vec{q} \cdot \vec{r}_j) \right]^2 \right\rangle + \left\langle \left[\sum_{j=1}^{N+1} \cos(\vec{q} \cdot \vec{r}_j) \right]^2 \right\rangle \right\}. \end{aligned} \quad (3)$$

Note that we have chosen here a normalization for which $S(q \rightarrow 0) = 1$. When a stretching force is applied to

one chain end in the +x-direction, the structure factor becomes anisotropic. In $d = 3$ dimensions, the confor-

mations of chains still have axis-symmetric geometries, and we must distinguish between $S_{||}(q_{||})$, where \vec{q} is oriented in the x-direction parallel to the force, and $S_{\perp}(\vec{q}_{\perp})$,

where \vec{q} is oriented perpendicular to it. So we define $\vec{r}_j = (x_j, y_j, z_j) = (x_j, \vec{\rho}_j)$ to obtain

$$S_{||}(q_{||}) = \frac{1}{(N+1)^2} \left\{ \left\langle \left[\sum_{j=1}^{N+1} \sin(q_{||} x_j) \right]^2 \right\rangle + \left\langle \left[\sum_{j=1}^{N+1} \cos(q_{||} x_j) \right]^2 \right\rangle \right\}, \quad (4)$$

$$S_{\perp}(q_{\perp}) = \frac{1}{(N+1)^2} \left\{ \left\langle \left[\sum_{j=1}^{N+1} \sin(\vec{q}_{\perp} \cdot \vec{\rho}_j) \right]^2 \right\rangle + \left\langle \left[\sum_{j=1}^{N+1} \cos(\vec{q}_{\perp} \cdot \vec{\rho}_j) \right]^2 \right\rangle \right\}. \quad (5)$$

Note that in $d = 2$ dimensions we have $\vec{r}_j = (x_j, y_j)$ and then $\vec{q}_{\perp} \cdot \vec{\rho}_j$ in Eq. (5) needs to be replaced simply by $q_{\perp} y_j$, of course.

We also stress that in this paper we are not at all concerned with effects due to the local structure of (effective) monomers, such as e.g. chemical side groups, etc.; such effects show up at large q when one considers the scattering from real chains [29]. We next define our notation for characteristic lengths of the chain. Assuming a rigidly fixed bond length ℓ_b between neighboring monomers along the chain, the contour length L is

$$L = N\ell_b \quad (6)$$

The mean square end-to-end distance (in the absence of stretching forces) simply is

$$\langle R^2 \rangle = \left\langle \left(\sum_{j=1}^N \vec{a}_j \right)^2 \right\rangle \quad (7)$$

with $\vec{a}_j = \vec{r}_{j+1} - \vec{r}_j$ being the j -th bond vector, and the mean square gyration radius is given by

$$\begin{aligned} \langle R_g^2 \rangle &= \frac{1}{N+1} \left\langle \sum_{j=1}^{N+1} (\vec{r}_j - \vec{r}_{CM})^2 \right\rangle \\ &= \frac{1}{(N+1)^2} \left\langle \sum_{j=1}^{N+1} \sum_{k=j+1}^{N+1} (\vec{r}_j - \vec{r}_k)^2 \right\rangle, \end{aligned} \quad (8)$$

where $\vec{r}_{CM} = \sum_{j=1}^{N+1} \vec{r}_j / (N+1)$ is the center of mass position of the polymer.

In the presence of stretching forces, the chain takes a mean extension $\langle X \rangle$ and mean square extensions also become anisotropic,

$$\langle X \rangle = \left\langle \sum_{j=1}^N a_{jx} \right\rangle, \quad \langle X^2 \rangle = \left\langle \left(\sum_{j=1}^N a_{jx} \right)^2 \right\rangle, \quad (9)$$

$$\langle R_{\perp}^2 \rangle = \left\langle \left(\sum_{j=1}^N a_{jy} \right)^2 \right\rangle + \left\langle \left(\sum_{j=1}^N a_{jz} \right)^2 \right\rangle. \quad (10)$$

Eq. (10) refers to the three-dimensional case, for $d = 2$ the second term in the right hand side needs to be omitted. A related anisotropy can then be stated for the gyration radius square as well, namely

$$\langle R_{g,||}^2 \rangle = \frac{1}{(N+1)^2} \left\langle \sum_{j=1}^{N+1} \sum_{k=j+1}^{N+1} (x_j - x_k)^2 \right\rangle, \quad (11)$$

$$\langle R_{g,\perp}^2 \rangle = \frac{1}{(N+1)^2} \left\langle \sum_{j=1}^{N+1} \sum_{k=j+1}^{N+1} [(y_j - y_k)^2 + (z_j - z_k)^2] \right\rangle, \quad (12)$$

for $d = 3$, again the term $(z_j - z_k)^2$ simply is omitted in the case $d = 2$.

We also recall that the mean square gyration radii describe the scattering functions at small \vec{q} . So in the absence of stretching forces we have

$$S(q) = 1 - q^2 \langle R_g^2 \rangle / d, \quad q \rightarrow 0, \quad (13)$$

while if stretching forces are present, one finds instead

$$S_{||}(q_{||}) = 1 - q_{||}^2 \langle R_{g,||}^2 \rangle, \quad q \rightarrow 0, \quad (14)$$

$$S_{\perp}(q_{\perp}) = 1 - q_{\perp}^2 \langle R_{g,\perp}^2 \rangle / (d-1), \quad q \rightarrow 0. \quad (15)$$

In addition to the limit $q \rightarrow 0$, also the limiting behavior of $S(q \rightarrow \infty)$ is trivially known: then all interference terms in Eq. (3) average to zero, and only the terms $j = k$ contribute to the double sum. Hence we obtain

$$\begin{aligned} S(q \rightarrow \infty) &= \frac{1}{N+1}, \\ S_{||}(q_{||} \rightarrow \infty) &= S_{\perp}(q_{\perp} \rightarrow \infty) = \frac{1}{N+1}, \end{aligned} \quad (16)$$

irrespective of the value of the persistence length ℓ_p , the value of an applied force f , etc.

At this point we emphasize, however, that it is not possible to write down a general definition for the persistence length ℓ_p that would be both universally valid and practically useful [10, 11, 13]. The definition often found in textbooks [6, 63] in terms of the asymptotic decay of the bond vector orientational function (of a very long chain, $N \rightarrow \infty$)

$$\langle \cos \theta(s) \rangle \equiv \langle \vec{a}_j \cdot \vec{a}_{j+s} \rangle / \langle \vec{a}_j \cdot \vec{a}_j \rangle \propto \exp(-s\ell_b/\ell_p), \quad s \rightarrow \infty \quad (17)$$

makes sense only for Gaussian PHANTOM chains, and is not applicable to real polymers under ANY CIRCUMSTANCES, since the asymptotic decay of $\langle \cos \theta(s) \rangle$ with the “chemical distance” $s\ell_b$ along the chain always is a power-law decay. In fact, for $\ell_p \ll s\ell_b \ll L$ one has [10, 11, 13, 64–67]

$$\langle \cos \theta(s) \rangle \propto s^{-\beta} \quad (18)$$

where $\beta = 3/2$ both in melts [64, 65] and for chains in dilute solution under Theta conditions [10, 66]. For the case of good solvent conditions, which is the problem of interest for the present paper, one rather finds the scaling law [10, 67]

$$\beta = 2(1 - \nu) \quad (19)$$

which yields $\beta = 0.825$ ($d = 3$) and $\beta = 1/2$ ($d = 2$), respectively. In simple cases, such as the semiflexible extension of the self-avoiding walk model studied in [13] and further investigated in the present work, one can rather use an analog of Eq. (17) but for short chemical distances,

$$\langle \cos \theta(s) \rangle = \exp(-s\ell_b/\ell_p), \quad 0 \leq s \leq \ell_p/\ell_b \quad (20)$$

Eq. (20) is useful for the simple model that will be studied in the present paper, namely the self-avoiding walk (SAW) on square and simple cubic lattices with an energy penalty ϵ_b for “bond bending” (i.e., kinks of the SAW by 90 degrees), which then serves as a convenient parameter to control the persistence length. Since for $\epsilon_b/k_B T < 2$ the power law, Eq. (18), already starts to set in even for small s of order unity already, we use in practice an alternative definition,

$$\ell_p/\ell_b = -1/\ln(\langle \cos \theta(1) \rangle), \quad (21)$$

which is equivalent to Eq. (20), if Eq. (20) holds over a more extended range of s . An alternative method considers the distribution function $P(n_{str})$ of n_{str} successive bond vectors \vec{a}_i having the same orientation without any kink, which is found to behave as [13] $P(n_{str}) = a_p \exp(-n_{str}/n_p)$, with a_p, n_p being constants. Both $\langle n_{str} \rangle$ and n_p can be taken as alternative estimates of a persistence length, and for large n_p these estimates agree with the result from Eq. (21) to within a relative accuracy of a few percent (or better), both in $d = 2$ and

in $d = 3$ dimensions [13]. Unfortunately, Eq. (21) is not straightforwardly applicable for chemically realistic models (such as alkane chains when ℓ_b means a bond between two successive carbon atoms, but the all-trans state corresponds to a zig-zag configuration with a nonzero bond angle $\theta(1)$). It also is not useful for coarse-grained models of polymers with complex architecture, such as bottle-brush polymers [10, 11]. Thus we emphasize that for our model Eq. (21) is a practically useful definition, while for real polymers studied experimentally the estimation of ℓ_p is a delicate problem. The same caveat applies for the Kuhn length ℓ_K , which is $\ell_K = 2\ell_p$ for worm-like chains, but the latter does not apply in solutions, as stated above. In dense melts, $\ell_K/\ell_b = 6\langle R_g^2 \rangle/(\ell_b^2 N)$ is supposed to hold, but due to local interactions with neighboring monomers in a dense environment it is not obvious that ℓ_K for a melt is a relevant parameter for a chain under good solvent conditions.

Thus, it is a clear advantage of our model calculations that via Eqs. (20), (21) accurate direct estimates of ℓ_p are possible, unlike in experiment. These estimates for ℓ_p are tabulated in Ref. [13].

B. Theoretical Predictions for the Scattering Function of Single Polymers in Good Solvents in the Absence of Stretching Forces

The classical result for the scattering from Gaussian chains is the well-known Debye function [1–4]

$$S_{\text{Debye}}(q) = \frac{2}{q^2 \langle R_g^2 \rangle} \left\{ 1 - \frac{1}{q^2 \langle R_g^2 \rangle} [1 - \exp(-q^2 \langle R_g^2 \rangle)] \right\} \quad (22)$$

Note that for large q this reduces to $S_{\text{Debye}}(q) \approx 2/(q^2 \langle R_g^2 \rangle)$, reflecting the random-walk like fractal structure of a Gaussian coil, $S_{\text{Debye}}(q) \propto q^{-1/\nu_{MF}}$ with $\nu_{MF} = 1/2$. Eq. (22) does not tell how large q can be in order for this power law to be still observable. For semiflexible Gaussian chains, the contour length $L = N\ell_b$ can be written as $L = n_p \ell_p$ and the mean square end-to-end distance and gyration radius are [14, 68]

$$\frac{\langle R^2 \rangle}{2\ell_p L} = 1 - \frac{1}{n_p} [1 - \exp(-n_p)], \quad (23)$$

$$\frac{6\langle R_g^2 \rangle}{2\ell_p L} = 1 - \frac{3}{n_p} + \frac{6}{n_p^2} - \frac{6}{n_p^3} [1 - \exp(-n_p)] \quad (24)$$

From Eqs. (23), (24) one can clearly recognize that Gaussian behavior of the radii is only seen if the number n_p of persistence lengths that fit to a given contour length of the chain is large, $n_p \gg 1$ (for n_p of order unity, a crossover to rod-like behavior occurs). Since q^{-1} also is a length scale, one concludes that the Gaussian coil behavior reflected in Eq. (22) also implies that a scale q^{-1} requires that a subchain with this gyration radius contains many persistence lengths as well, i.e. Eq. (22) can

only hold for

$$q\ell_p \ll 1. \quad (25)$$

In the regime

$$\ell_p^{-1} \ll q \ll \ell_b^{-1} \quad (26)$$

we expect that the scattering function will resemble the scattering function of a rigid rod of length L_{rod} [69]

$$S_{\text{rod}}(q) = \frac{2}{qL_{\text{rod}}} \left[\int_0^{qL_{\text{rod}}} dx \frac{\sin x}{x} - \frac{1 - \cos(qL_{\text{rod}})}{qL_{\text{rod}}} \right], \quad (27)$$

which for large q varies like

$$S_{\text{rod}}(q \rightarrow \infty) = \pi/(qL_{\text{rod}}). \quad (28)$$

Note that Eqs. (27), (28) refer to a rigid rod on which the scattering centers are uniformly and continuously distributed. In the lattice model that is studied here, the scattering centers are just the subsequent lattice sites along the rod, and since for a rod of length L_{rod} there are then $L_{\text{rod}} + 1$ such scattering centers, one has [70]

$$S_{\text{rod}}(q) = \frac{1}{L_{\text{rod}} + 1} \left[-1 + \frac{2}{L_{\text{rod}} + 1} \sum_{k=0}^{L_{\text{rod}}} (L_{\text{rod}} + 1 - k) \frac{\sin qk}{qk} \right], \quad q < \pi. \quad (29)$$

Both Eqs. (27), (29) have a simple smooth crossover from $S_{\text{rod}}(q) = 1 - q^2 \langle R_g^2 \rangle_{\text{rod}}/3$ with $\langle R_g^2 \rangle_{\text{rod}} = L_{\text{rod}}^2/12$ to the $1/q$ power law (Eq. (28)). Of course, on the lattice consideration of $q > \pi$ does not make sense, since distances of the order of a lattice spacing and less are not meaningful.

While for a Gaussian coil no direction of \vec{q} is singled out, for a rod it makes sense to consider also the special case where the wave vector \vec{q} is oriented along the rod; rather than considering the case when all orientations of q are averaged over, as done in Eqs. (27) - (29). Then one rather obtains, q_{\parallel} being the component of \vec{q} parallel to the axis of the rod [56]

$$S_{\text{rod}}(q_{\parallel}) = \frac{2}{(q_{\parallel}L_{\text{rod}})^2} [1 - \cos(q_{\parallel}L_{\text{rod}})]. \quad (30)$$

Note that Eq. (30) leads to an oscillatory decay since $\cos(q_{\parallel}L_{\text{rod}}) = 1$ for $q_{\parallel}^{(k)} = k(2\pi/L_{\text{rod}})$, $k = 0, 1, 2, \dots, L_{\text{rod}}$, and $S_{\text{rod}}(q_{\parallel})$ hence has zeros for all $q_{\parallel}^{(k)}$, $k = 0, 1, 2, \dots, L_{\text{rod}}$.

When we consider the scattering from semiflexible Gaussian chains, we now expect a smooth crossover between the Debye function, $S_{\text{Debye}}(q)$ and the rod scattering, Eq. (27), similar to the smooth crossovers from rods to Gaussian coils, as described for the radii by Eqs. (23) and (24). It turns out that this is a formidable problem, and no simple explicit formula exists, despite the fact that excluded volume effects still are neglected [17–21, 23–33, 35, 37–39]. Kholodenko [32] derived an interpolation formula which describes the two limiting cases of Gaussian coils and rigid rods exactly, and which is expected to show only small deviations from the exact result in the intermediate crossover regime. His result

can be cast in the form

$$S(q) = \frac{2}{x} [I_1(x) - \frac{1}{x} I_2(x)], \quad x = 3L/2\ell_p \quad (31)$$

where

$$I_n(x) = \int_0^x dz z^{n-1} f(z), \quad (32)$$

and the function $f(z)$ is given by

$$f(z) = \begin{cases} \frac{1}{E} \frac{\sinh(Ez)}{\sinh z}, & q \leq \frac{3}{2\ell_p}, \\ \frac{1}{E} \frac{\sin(Ez)}{\sin z}, & q > \frac{3}{2\ell_p}, \end{cases} \quad (33)$$

with

$$E = \left[1 - \left(\frac{2q\ell_p}{3} \right)^2 \right]^{1/2}, \quad \hat{E} = \left[\left(\frac{2q\ell_p}{3} \right)^2 - 1 \right]^{1/2}. \quad (34)$$

In addition, Stepanow [35] has developed a systematic expansion of the scattering function in terms of the solution for the quantum rigid rotator problem, which converges fast if L/ℓ_p is not too large. Note that the opposite limit, $L/\ell_p \rightarrow \infty$, has already been considered by des Cloizeaux [23], and his result has been quoted in the introduction (Eq. (1)). This expansion (as well as equivalent representations written as continued fractions [33]) can only be evaluated numerically [71].

However, a few qualitative statements can be made on the structure factor $S(q)$ in the representation of a Kratky plot, $qLS(q)$ plotted vs. Lq . While Eqs (27)–(29) imply a monotonous increase from the straight line $qLS(q \approx 0) = qL$ towards the plateau value $qLS(q \gg$

$2\pi/L) = \pi$ for simple rigid rods, for semiflexible polymers this Kratky plot exhibits a maximum, since in the regime of interest we may crudely approximate $S(q)$ by its leading terms

$$qLS(q) \approx qL - \frac{1}{3}(qL)^3 \frac{\langle R_g^2 \rangle}{L^2}. \quad (35)$$

$$q_{\max} = 1/\sqrt{\langle R_g^2 \rangle}, \quad q_{\max}LS(q_{\max}) = \frac{2}{3}L/\sqrt{\langle R_g^2 \rangle} \quad (36)$$

i.e. From Eqs. (35), (24) we immediately find, for $n_p \gg 1$,

$$q_{\max} = \sqrt{3/(\ell_p L)}, \quad q_{\max}LS(q_{\max}) = \frac{2}{\sqrt{3}}\sqrt{L/\ell_p}. \quad (37)$$

Using the full Debye function one finds a different prefactor, $q_{\max} \approx \sqrt{6.4/(\ell_p L)}$, but the general scaling behavior is the same as given by Eq. (37). Thus, when L is known (as is the case in simulations) for semiflexible Gaussian chains estimation of the coordinates of the maximum in the Kratky plot allows a straightforward estimation of the persistence length ℓ_p .

Considering now the effects of excluded volume, we emphasize that Eq. (36) still is supposed to be valid, while Eq. (37) no longer holds. In particular, in Ref. [13] it was shown that in $d = 2$ the Kratky-Porod model [14] of semiflexible chains, on which Eqs. (23), (24), and (31)-(34) are based, has no validity whatsoever: rather it was shown that around $n_p = 1$ a smooth crossover from the rigid rod behavior to the behavior of two-dimensional self-avoiding walks occurs. Thus, we expect similarly instead of Eq. (24) that (recall $n_p = L/\ell_p$)

$$\frac{\langle R_g^2 \rangle}{\ell_p L} = f(n_p), \quad \text{with} \quad f(n_p < 1) = n_p, \quad (38)$$

as in Eq. (24), but

$$f(n_p \gg 1) = C_g^s n_p^{2\nu_2 - 1}, \quad \nu_2 = 3/4, \quad (39)$$

C_g^s being (for $\ell_p/\ell_b \gg 1$) a non-universal constant. Eqs. (38), (39) hence imply in $d = 2$ dimensions

$$\langle R_g^2 \rangle = C_g^s \ell_p^{1/2} L^{3/2}, \quad L \rightarrow \infty, \quad (40)$$

in full analogy to the result for fully flexible chains,

$$\langle R_g^2 \rangle = C_g^f \ell_b^{1/2} L^{3/2}, \quad L \rightarrow \infty, \quad (41)$$

where C_g^f is another non-universal constant. Similar relations were found [13] for the end-to-end distance

$$\begin{aligned} \langle R^2 \rangle &= C_e^f \ell_b^{1/2} L^{3/2} \text{ (flexible)}, \\ \langle R^2 \rangle &= C_e^s \ell_p^{1/2} L^{3/2} \text{ (semiflexible)} \end{aligned} \quad (42)$$

with C_e^f and C_e^s other (non-universal) constants for flexible and semiflexible chains, respectively. The ratios

C_e^f/C_g^f and C_e^s/C_g^s are expected to be universal, however (for Gaussian chains $\langle R_e^2 \rangle/\langle R_g^2 \rangle = 6$), for both flexible and semiflexible chains.

In $d = 3$ dimensions, however, the situation in the presence of excluded volume is considerably more involved [13]. For the end-to-end distance $\langle R^2 \rangle$ of semiflexible chains, two successive crossovers were found: for $n_p \approx 1$ a crossover from rods to Gaussian coils occur, while excluded volume effects become prominent for

$$n_p > n_p^*, \quad n_p^* \propto (\ell_p/D)^\zeta \quad (43)$$

where we have introduced the chain diameter D as another characteristic length that may be needed in general (while in our model $D = \ell_b$, however), and ζ is an exponent that is not yet known precisely. Arguments based on Flory theory yield [13, 15, 16] $\zeta = 2$ while Monte Carlo results rather suggested [13] $\zeta \approx 1.5$. We recall that in $d = 3$ Flory arguments are not [1] exact, implying [3, 9] $\nu = 3/5$ instead of $\nu = 0.588$. A similar double crossover from rods to first Gaussian coils and then to $d = 3$ self-avoiding walks is expected to be visible in $\langle R_g^2 \rangle$, too. If we could rely on Flory theory, we would predict from these considerations that

$$\langle R_g^2 \rangle/(\ell_p L) = C_g^s (n_p/n_p^*)^{2\nu-1}, \quad n_p > n_p^* \quad (44)$$

and hence (using the Flory value $\nu = 3/5$)

$$\langle R_g^2 \rangle = C_g^s L^{6/5} (\ell_p D)^{2/5}. \quad (45)$$

From $q_{\max} = (\sqrt{C_g^s} L^{3/5} (\ell_p D)^{1/5})^{-1}$ the persistence length ℓ_p can be inferred, provided C_g^s has been determined. However, if $\ell_p \gg \ell_b$ and $D = \ell_b$, one can study the regime $1 < n_p < n_p^*$, where Gaussian statistics for the gyration radius is still applicable, and hence Eq. (37) applies.

C. The structure factor in the presence of stretching forces

For Gaussian chains under stretch, where a force f is applied at a chain at one end in the $+x$ -direction, the other end being fixed at the coordinate origin, the structure factor $S(\vec{q})$ has been derived by Benoit et al. [40] as follows $\{\vec{q} = (q_x, q_y, q_z)$ with $q_{||} = q_x$ and $q_{\perp} = \sqrt{q_y^2 + q_z^2}\}$

$$S_{||}(q_{||}) = 2Re \left\{ \frac{\exp(-X_{||}) - 1 + X_{||}}{X_{||}^2} \right\}, \quad (46)$$

$$S_{\perp}(q_{\perp}) = 2 \frac{\exp(-X_{\perp}) - 1 + X_{\perp}}{X_{\perp}^2}, \quad (47)$$

where $X_{\perp} = q_{\perp}^2 (\langle R^2 \rangle_0 / 6\lambda_{\perp}^{-2})$, with $\langle R^2 \rangle_0$ the mean-square end-to-end distance of the chain in the absence

of any force ($f = 0$), and λ_\perp describes the modification of the Gaussian distribution in the transverse directions (y and z -direction, for $d = 3$). The quantity X_\parallel is complex (therefore the real part of Eq. (46) is taken) and is given by

$$X_\parallel = \frac{q_\parallel^2 \langle R^2 \rangle_0}{6\lambda_\parallel^{-2}} + i\langle X \rangle q_\parallel \quad (48)$$

where λ_\parallel describes the modification of the Gaussian distribution in the x -direction (parallel to the force). Benoit et al. [40] explicitly state that their result is restricted to deformations of small amplitudes, and do not specify how λ_\perp , λ_\parallel are related to the applied force. However, considering the small q expansion of Eqs. (46), (47) one can relate these parameters to the mean square gyration radius components of the chain, since for $X_\perp \ll 1$

$$S(q_\perp) = 1 - q_\perp^2 \frac{\langle R^2 \rangle_0}{18\lambda_\perp^{-2}} = 1 - q_\perp^2 \langle R_{g,\perp}^2 \rangle / 2, \quad (49)$$

where in the last step Eq. (15) was used. Hence we conclude (note that $\langle R_g^2 \rangle_0 = \langle R^2 \rangle_0 / 6$ for Gaus-

sian chains) that $\lambda_\perp^2 = (3/2)\langle R_{g,\perp}^2 \rangle / \langle R_g^2 \rangle_0 = (\langle R_{gy}^2 \rangle + \langle R_{gz}^2 \rangle) / (\langle R_{gy}^2 \rangle_0 + \langle R_{gz}^2 \rangle_0)$, as expected. Similarly, Eq. (46) yields for $q_\parallel \rightarrow 0$, using also Eq. (14)

$$S(q_\parallel) = 1 - q_\parallel^2 \left(\frac{\langle R^2 \rangle_0}{18\lambda_\parallel^{-2}} + \frac{\langle X \rangle^2}{12} \right) = 1 - q_\parallel^2 \langle R_{g,\parallel}^2 \rangle, \quad (50)$$

and hence we see that λ_\parallel in X_\parallel can be expressed in terms of the gyration radius component $\langle R_{g,\parallel}^2 \rangle$ of the stretched chain and the extension $\langle X \rangle$. However, since from the work of Benoit et al. [40] it is not clear that Eqs. (46), (47) are applicable for conditions where $\langle X \rangle / L$ is not very small, we hence rederived Eqs. (46), (47) by an independent method, which is more transparent with respect to the basic assumptions that are made. This derivation is presented in an Appendix, and it shows that $S(q_\parallel)$ can be cast into the form

$$S(q_\parallel) = \frac{1}{(N+1)^2} \sum_{i,j} \exp \left[-\frac{1}{2} q_\parallel^2 (\langle X^2 \rangle - \langle X \rangle^2) \frac{|i-j|}{N} \right] \cos \left(q_\parallel \frac{|i-j| \langle X \rangle}{N} \right) \quad (51)$$

which is equivalent to Eq. (46) but with a somewhat different expression for X_\parallel , namely

$$X_\parallel = \frac{1}{2} q_\parallel^2 (\langle X^2 \rangle - \langle X \rangle^2) + i q_\parallel \langle X \rangle. \quad (52)$$

It is interesting to note that Eqs. (46) and (51) can be given a very simple physical interpretation: with respect to the correlation in stretching direction, the stretched polymers is equivalent to a harmonic one-dimensional “crystal” (which at nonzero temperature lacks long range order, of course) of length $Na = \langle X \rangle$, a being the “lattice spacing” of the crystal.

Writing the Hamiltonian of the one dimensional chain as [72, 73]

$$\mathcal{H} = \frac{1}{2} \sum_\ell \left[\frac{\pi_\ell^2}{m} + mc^2 \frac{(x_{\ell+1} - x_\ell - a)^2}{a^2} \right], \quad (53)$$

where point particles of mass m have positions x_ℓ and conjugate momenta π_ℓ , and the spring potential coupling neighboring particles is written in terms of the sound velocity c . At $T = 0$, particles would be localized at positions $x_n^{(0)} = x_0^{(0)} + na$, $n = 0, 1, \dots, N$. So it makes sense to consider displacements relative to the ground state, $u_n = x_n - x_n^{(0)} = x_n - na$, putting $x_0^{(0)}$ at the

origin. Due to the harmonic character of this “crystal”, one can calculate the mean square displacements easily to find (assuming periodic boundary conditions) that $\langle (u_n - u_0)^2 \rangle = na^2 k_B T / (mc^2) = n\delta^2$, where δ characterizes the local displacement for two neighboring particles. Applying the formula also for the end-to-end distance of a chain without periodic boundary conditions, $\langle (u_N - u_0)^2 \rangle = N\delta^2$, one immediately finds that $S(q_\parallel)$ for the harmonic chain yields the above expressions of $S(q_\parallel)$, since $X = x_N - x_0 = Na + u_N - u_0$, $\langle X \rangle = Na$, and $\langle X^2 \rangle = N^2 a^2 + N\delta^2 = \langle X \rangle^2 + N\delta^2$. This consideration also emphasizes that a condition $\langle X \rangle \ll L = N\ell_b$ in fact is not required for the validity of Eqs. (46)-(52).

For the unstretched case ($\langle X \rangle = 0$) Eqs. (46)-(52) reduce to Eq. (22), as it should be. We recall that according to the Kratky-Porod model simple approximations for the extension $\langle X \rangle$ of a chain as a function of the force can be derived (see [13] for a review), namely

$$\frac{f\ell_p}{k_B T} = \frac{3}{4} \frac{\langle X \rangle}{L} + \frac{1}{8(1 - \langle X \rangle / L)^2} - \frac{1}{8}, \quad d = 2, \quad (54)$$

and

$$\frac{f\ell_p}{k_B T} = \frac{3}{4} \frac{\langle X \rangle}{L} + \frac{1}{4(1 - \langle X \rangle / L)^2} - \frac{1}{4}, \quad d = 3. \quad (55)$$

TABLE I: Values of persistence lengths ℓ_p/ℓ_b for semiflexible chains in $d = 2$ and $d = 3$, estimated by Eq. (21), and the crossover length N^* between the intermediate Gaussian regime and the SAW regime in $d = 3$, estimated empirically from Fig. 7b of Ref. [13] ($N^* = N^{\text{rod}} = 2\ell_p/\ell_b$ in $d = 2$) for various values of q_b .

q_b	0.005	0.01	0.02	0.03	0.05	0.10	0.20	0.40	1.0
$\ell_p/\ell_b(d = 2)$	118.22	59.44	30.02	20.21	12.35	6.46	3.50	2.00	1.06
$\ell_p/\ell_b(d = 3)$	51.52	26.08	13.35	9.10	5.70	3.12	1.18	1.12	0.67
$N^*(d = 3)$	36000	9000	1850	700	180	41	11	-	-

Eqs. (54), (55) imply in the linear response regime, where $\langle X \rangle \propto f$, that

$$\frac{f\ell_p}{k_B T} = \frac{d\langle X \rangle}{2L}. \quad (56)$$

However, from linear response one can show generally that

$$\langle X \rangle = f\langle X^2 \rangle_0 / (k_B T) = f\langle R^2 \rangle_0 / (dk_B T), \quad (57)$$

where $\langle R^2 \rangle_0$ is the mean square end-to-end distance in the absence of forces. Eqs. (56), (57) are compatible with each other for Gaussian semiflexible chains, for which $\langle R^2 \rangle_0 = 2\ell_p L$ {Eq. (23)}, but are incompatible in the presence of excluded volume forces. In this case, one observes a crossover from the linear response regime, as described by Eq. (57) together with Eq. (42) for $d = 2$ and a result analogous to Eq. (55), namely

$$\langle R_e^2 \rangle = C_e^s L^{6/5} (\ell_p D)^{2/5}, \quad d = 3 \text{ (using } \nu \approx 3/5), \quad (58)$$

to the so-called ‘‘Pincus blob’’ [41] regime, described by a power law for the extension versus force relation

$$\langle X \rangle / L \propto (f\ell_p / k_B T)^{1/\nu-1}. \quad (59)$$

While in $d = 2$ Eq. (57) holds up to $\langle X \rangle / L$ of order unity, where then saturation effects ($\langle X \rangle / L \rightarrow 1$ for large enough f) set in, in $d = 3$ the regime of validity of Eq. (57) is much more restricted, namely we have to require [13]

$$\xi_p \equiv k_B T / f > R_0 \propto \ell_p^2 / D \quad (60)$$

For stronger forces (corresponding to $\xi_p < R_0$) the Kratky-Porod results, Eqs. (54), (55), are expected to become valid. In the Pincus blob regime, also nontrivial power laws for the fluctuations $\langle X^2 \rangle - \langle X \rangle^2$ and the transverse linear dimensions are predicted [54]

$$\langle X^2 \rangle - \langle X \rangle^2 \propto \langle R_{\perp}^2 \rangle \propto (f\ell_p / k_B T)^{1/\nu-2}. \quad (61)$$

Since we are not aware of any treatment of the structure factor of the Kratky-Porod model under stretch, we shall use Eqs. (46), (47) also for semiflexible chains (but using the numerical results for $\langle X \rangle$ and $\langle X^2 \rangle - \langle X \rangle^2$, $\langle R_{g,\perp}^2 \rangle$, rather than theoretical predictions).

III. MODEL AND SIMULATION TECHNIQUE

Our model is the standard self-avoiding walk (SAW) on the square and simple cubic lattices, effective monomers being described by occupied lattice sites, connected by bonds. Each site can be taken only once, and thus we realize the excluded volume interaction. The lattice spacing henceforth is our unit of length, $\ell_b = 1$. We introduce an energy ϵ_b for any kink the walk takes (by an angle of $\pm 90^\circ$). Any such kink introduces hence a factor $q_b = \exp(-\epsilon_b / k_B T)$ to the statistical weight of the walk.

In the presence of a force f coupling to the extension X of the chain in x-direction, the statistical weight gets another factor b^X , with $b = \exp(f / k_B T)$. Then the partition function of a SAW with N bonds (i.e., $N+1$ effective monomers) and N_{bend} local kinks becomes

$$Z_{N, N_{\text{bend}}}(q_b, b) = \sum_{\text{config.}} C(N, N_{\text{bend}}, X) q_b^{N_{\text{bend}}} b^X \quad (62)$$

By the pruned-enriched Rosenbluth method (PERM) it is possible to obtain estimates of the partition function and quantities derived from it (e.g. $\langle X \rangle$, $\langle X^2 \rangle$) and additional averages such as $S(q)$, using chain lengths up to $N = 25600$. Both the chain stiffness and the force f have been varied over a wide range; for $q_b = 1$ one has fully flexible self-avoiding random walks, while for $q_b = 0.005$ the persistence length (computed from Eq. (21)) is of the order of 120 in $d = 2$ and 52 in $d = 3$ (Table I lists our corresponding estimates). For technical details on the implementation of the algorithm, we refer to the literature [13].

IV. RESULTS FOR THE SCATTERING FUNCTION OF UNSTRETCHED CHAINS

We start with our data for the mean square gyration radius $\langle R_g^2 \rangle$, normalized by the square of the Kuhn length $\ell_K = 2\ell_p$, plotted vs. the number of Kuhn segments $n_K = L/\ell_K = N\ell_b/(2\ell_p)$, Fig. 1a since this was the representation chosen for the experimental data of Norisuye and Fujita [12], which we reproduce in Fig. 1b. Both diagrams show the same range of abscissa ($30 \leq n_K \leq 3000$) and ordinate ($5 < \langle R_g^2 \rangle / (2\ell_p)^2 < 1000$). The qualitative similarity between both simulation and experiment is striking. Since only the regime of rather large n_K is shown, the crossover from rods to Gaussian chains is not included

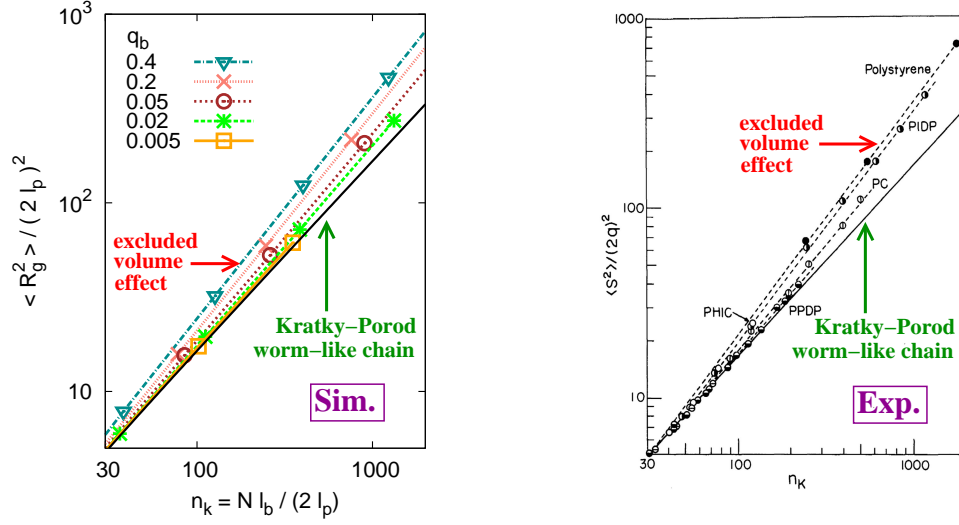


FIG. 1: (a) Log-log plot of normalized gyration radius square $\langle R_g^2 \rangle / (2\ell_p)^2$ versus the number of Kuhn segments, for the range $30 \leq n_K \leq 3000$, for chains of widely varying stiffness, and comparison to corresponding experimental data (b), taken from Norisuye and Fujita [12]. The full straight line is the Kratky-Porod model, Eq. (24).

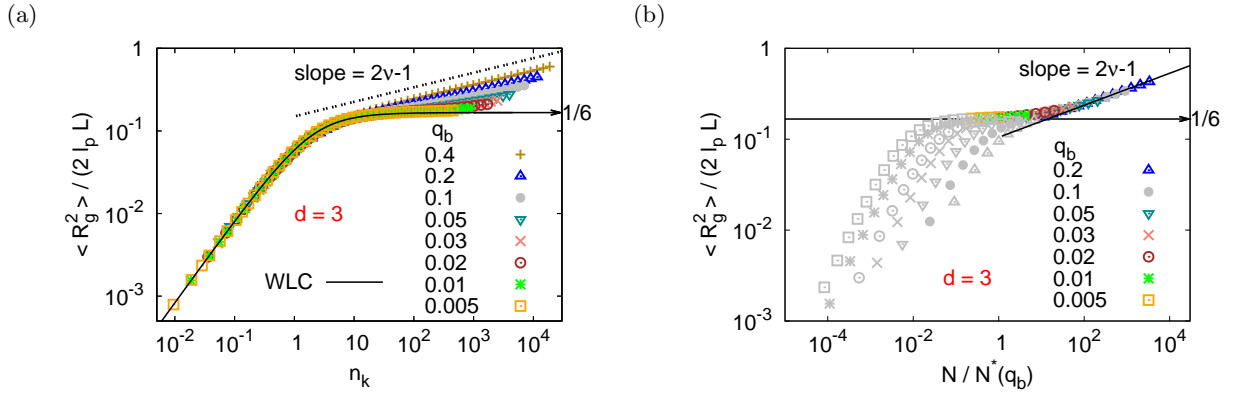


FIG. 2: (a) Log-log plot of $\langle R_g^2 \rangle / (2\ell_p L)$ versus n_K for $d = 3$, and including data for widely varying persistence lengths. Note that the worm-like chain result, WLC (Eq. (24)), describes correctly the crossover from rods to coils, but not the onset of excluded volume effects. (b) Same as (a), but choosing $N/N^*(q_b)$ as an abscissa variable ($N^*(q_b)$ was already estimated for a similar scaling plot for the mean square end-to-end distance, cf. Fig. 7b of Ref. [13]). Here $L = N\ell_b$.

(the full straight line represents the Gaussian chain behavior, as described by Eq. (24) for $n_K = (1/2)n_p \gg 1$). One can see that Eq. (24) works for very stiff chains and not too large n_K , while for large n_K systematic deviations occur, which can be attributed to excluded volume effects. Both the simulation and the experiment include data for widely varying persistence lengths (in the experiment, this could only be achieved by combining data for chemically different polymers in this plot). From their results (see Fig. 1b) the experimentalists concluded that the excluded volume effects set in for $n_K > 50$, irrespective of the precise value of the persistence length.

However, this latter conclusion needs to be questioned: in fact, for large n_K the data do not superimpose in

this representation for different choices of ℓ_p , indicating that the behavior is more complicated. To elucidate this, we take out the leading power law in the Gaussian coil regime, plotting $\langle R_g^2 \rangle / (\ell_p L)$ versus n_K over the full range (Fig. 2a). One sees that nice scaling behavior occurs with respect to the crossover from rigid rods to Gaussian coils; in this regime, Eq. (24) works in $d = 3$. However, now one can see rather clearly that the crossover from Gaussian coils to SAWs does not scale in this representation: rather for large n_K the curves “splay out”, the larger ℓ_p the longer the data follow Eq. (24), before an onset of excluded volume effects can be seen. This behavior has already been studied in Ref. [13] with respect to the end-to-end distance. Empirically, it was found that scal-

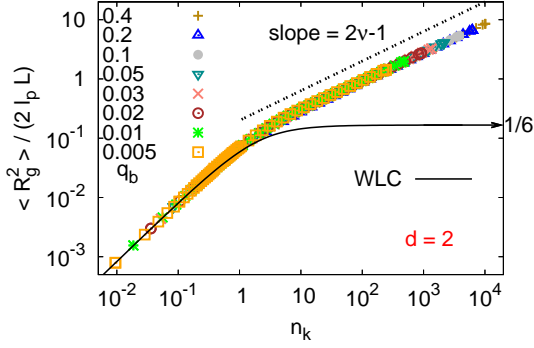


FIG. 3: Log-log plot of $\langle R_g^2 \rangle / (2\ell_p L)$ versus n_K for $d = 2$, including data for widely varying persistence lengths. Note that in $d = 2$ there occurs a direct crossover from rods to SAWs, an intermediate Gaussian regime is absent.

ing N with N^* , where $N^* \propto \ell_p^{2.5}$ rather than $N^* = \ell_p$. Fig. 2b shows that a master curve results as an envelope of the curves for individual ℓ_p . We also recall, that Flory arguments predict $N^* \propto \ell_p^3$, cf. Eq. (43) and the subsequent discussion. The data in Fig. 2 are fully analogous to our data on the end-to-end distance that were discussed recently elsewhere [13]. In $d = 2$, however, the behavior is clearly simpler (Fig. 3): there occurs a single crossover from rods to $d = 2$ SAWs, and a regime where the Kratky-Porod worm-like chain model presents a faithful description of the data is absent. These results for $\langle R_g^2 \rangle$ confirm our earlier analogous findings [13] for $\langle R_e^2 \rangle$.

Fig. 4 shows some of our raw data for the structure factor $S(q)$. For small q , one recognizes the Guinier regime, $S(q) \approx \exp(-q^2 \langle R_g^2 \rangle / 3) \approx 1 - q^2 \langle R_g^2 \rangle / 3$, and then a crossover occurs to the power law of SAWs or of Gaussian chains (the latter is seen clearly only for $d = 3$ and very stiff chains). At large q and stiff chains, the expected q^{-1} behavior is in fact compatible with the data.

It turns out that an analysis of $S(q)$ in the form of Kratky plots (Eq. (35)) is more illuminating, cf. Fig. 5: The location of the maximum in the Kratky plot, as discussed in Eqs. (36), (37), is easily identified, and it shows the expected scaling with L/ℓ_p both in $d = 3$ and in $d = 2$ (Fig. 6). In $d = 3$, one notes that with increasing L/ℓ_p a crossover from Gaussian behavior to SAW behavior occurs. Our data also confirm that for rather stiff chains in $d = 3$ both the Kholodenko and the Stepanow theories describe $S(q)$ very accurately. Note that Fig. 5b refers to rather short chains, for which strong effects due to excluded volume interactions are not yet expected, and hence the good agreement with the theories is not surprising.

Another issue of interest is the behavior $qLS(q)$ in the rigid rod limit, where one clearly notes the approach to π (Fig. 5). Can we then use $S(q)$ in this region, applying the des Cloizeaux formula {Eq. (1)} to extract quanti-

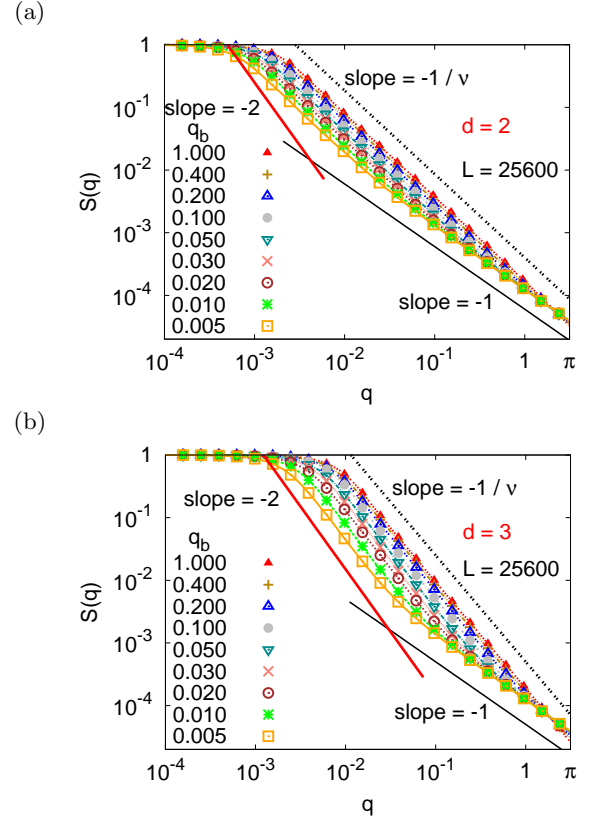


FIG. 4: Structure factor $S(q)$ plotted q , on log-log scales, for $d = 2$ (a) and $d = 3$ (b); only data for $L = 25600$ are shown, but many different choices of the stiffness parameter q_b are included. The straight lines indicate the rod-like behavior at large q (slope = -1) and the SAW behavior for flexible chains (slope = $-1/\nu$). Also the slope expected in the Gaussian regime is included (slope = -2). Only data up to $q = \pi$ have been included (larger q cannot be studied due to the lattice character of our model).

tatively reliable estimates for the persistence length ℓ_p from a plot of $qLS(q)$ versus $1/q$? Fig. 7 suggests that although a regime occurs where the variation is linear in $(q\ell_p)^{-1}$, the coefficient of this linear variation is inconsistent with the des Cloizeaux result. We have no final answer to offer to explain this discrepancy; we suspect that in the regime where q^{-1} and ℓ_p are of the same order, the discreteness of our lattice model (opposed to the Kratky-Porod continuum model) might matter.

V. RESULTS FOR THE SCATTERING FUNCTION OF CHAINS UNDER STRETCH

While for unstretched chains it is only $\langle R_g^2 \rangle$ as a measure of the linear dimension of the whole chain which is relevant (Figs. 1-3), for chains under the action of stretching forces anisotropy of the conformation of the chain comes into play. However, from the small q expansion of Eqs. (4), (5) one can show straightforwardly

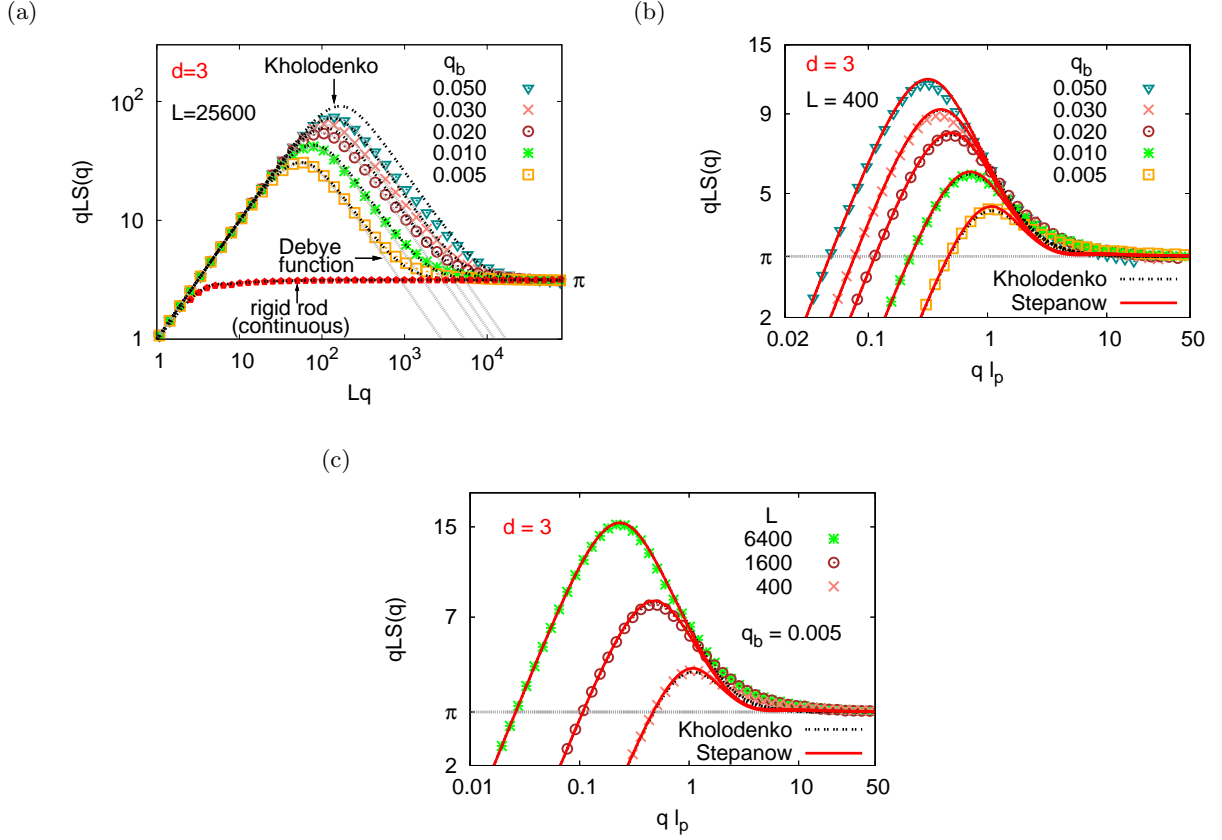


FIG. 5: (a) Rescaled structure factor $qLS(q)$ plotted against Lq for $d = 3$ and $L = 25600$, including 5 choices of the stiffness. The result for Gaussian chains (Debye function) and for continuous rigid rods (for which $qLS(q) \rightarrow \pi$ for large q . cf. Eq. (28)) are included for comparison. Also predictions obtained from the formulas proposed by Kholodenko {Eqs. (31)-(34)} are shown. (b) Rescaled structure factor $qLS(q)$ plotted against $q\ell_p$ for $d = 3$ and for $L = 400$, including both the predictions due to Stepanow [34] and Kholodenko {Eq. (31) - (34)}, which are essentially indistinguishable on the scale of the figure. (c) Same as (b), but for 3 different choices of L for $q_b = 0.005$.

that $S_{||}(q_{||})$ yields information on $\langle R_{g,||}^2 \rangle$ and $S_{\perp}(q_{\perp})$ on $\langle R_{g,\perp}^2 \rangle$ cf. Eqs. (14) and (15). Since for larger $q_{||}$ where also the extension $\langle X \rangle$ of the chain along the direction of the force enters the description of the scattering, we begin with a discussion of these linear dimensions and describe their variation as a function of the force f (for a more detailed discussion and related results, we refer the reader to Ref. [13]).

Fig. 8 shows typical data of $\langle R_{g,\perp}^2 \rangle$ versus $f\ell_p/k_B T$, both for rather flexible chains ($q_b = 0.4$) and for rather stiff chains ($q_b = 0.01$ in $d = 2$, $q_b = 0.05$ in $d = 3$, respectively). We recognize three regimes: for very small forces $\langle R_{g,\perp}^2 \rangle \approx \langle R_{g,\perp}^2 \rangle_0$, the unperturbed value in the absence of forces. In this linear response regime, the force orients the coil without deforming it. Then we recognize a regime where $\langle R_{g,\perp}^2 \rangle$ decreases according to a power law, namely Eq. (61). This power law holds in the regime where the radius of the Pincus blob, $\xi_p = k_B T/f$, is smaller than the unperturbed radius, but much larger than the persistence length ℓ_p itself. Thus this is the analog of the ‘‘Pincus blob’’ law that yields another power

law for the extension vs. force curve, Eq. (59). The physical picture invoked here for the chain is an elastic string of Pincus blobs, $\langle R_{g,\perp}^2 \rangle$ describing the mean square displacement of this string in transverse directions. As one can see from Fig. 8, the data indeed are compatible with the predicted power law in $d = 2$, and in $d = 3$ at least for the flexible chains. For stiff chains in $d = 3$, the regime where Eq. (61) holds is more restricted, since the Kratky-Porod regime has a more extended regime of validity, effects due to Pincus blobs can only be detected in a regime $\langle R_{g,\perp}^2 \rangle_0^{1/2} > \xi_p > R^* \propto \ell_p^2/D$, cf. Eq. (60) [13]. Therefore we have not included very stiff chains in Fig. 8b (for $q_b = 0.005$, leading to $\ell_p \approx 52\ell_b$, excluded volume effects, which also are responsible for the existence of Pincus blobs, could even for chains as long as $N = 25600$ hardly be detected in the chain linear dimensions in the absence of a force, cf. Figs. 1-3). So this failure to detect Pincus blobs for very stiff long chains in $d = 3$ dimensions is hardly surprising (although Eq. (61) ultimately will become valid as $N \rightarrow \infty$, irrespective how large ℓ_p is).

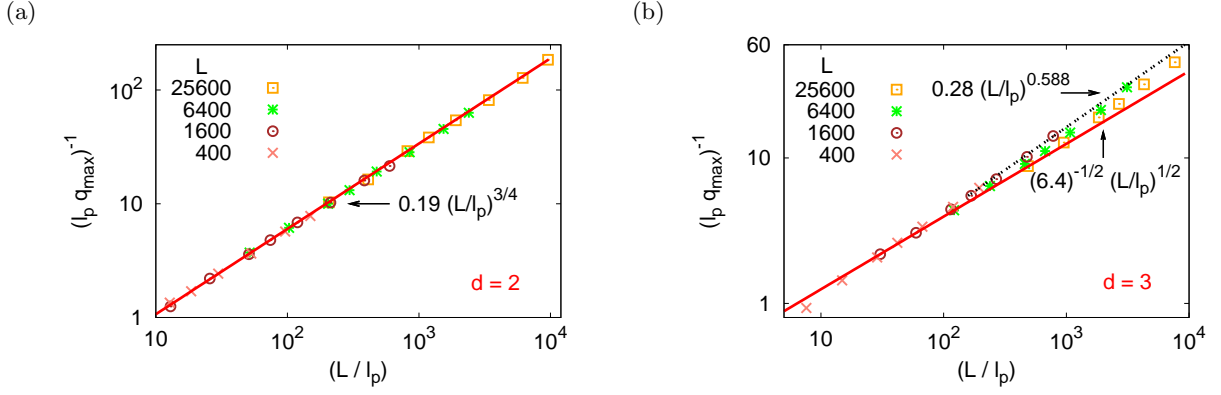


FIG. 6: Log-log plot of the inverse position of the maximum in the Kratky plot, $(\ell_p q_{\max})^{-1}$, versus the rescaled contour length L/ℓ_p , for $d = 2$ (a) and $d = 3$ (b). The full straight line included in (a) is described by the equation $0.19(L/\ell_p)^{3/4}$. In case (b), two straight lines with slope $\nu = 1/2$ and $\nu = 0.588$ are included, to illustrate the crossover. In both cases the persistence length ℓ_p is varied over a wide range, and the contour lengths chosen are $L = 400, 1600, 6400$ and 25600 , as indicated.

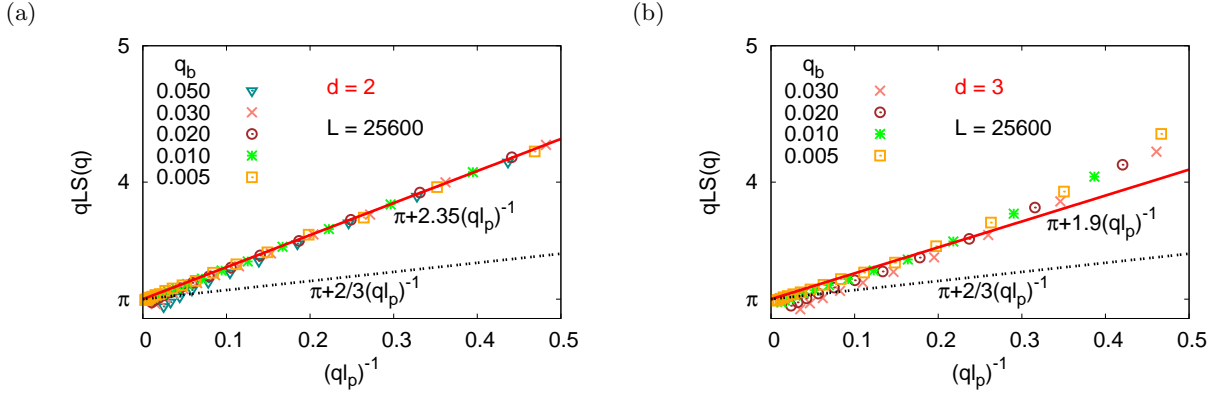


FIG. 7: Plot of $qLS(q)$ vs. $(qL_p)^{-1}$, for $d = 2$ (a) and $d = 3$ (b). All data are for $L = 25600$ only, and many different choices of q_b , as indicated. In each case, two straight lines are shown: the result of des Cloizeaux [23], Eq. (1), $qLS(q) = \pi + (2/3)(q\ell_p)^{-1}$, and empirical fits, $qLS(q) = \pi + 2.35(q\ell_p)^{-1}$ for $d = 2$ and $qLS(q) = \pi + 1.9(q\ell_p)^{-1}$ for $d = 3$, respectively.

Another interesting behavior is the apparent power law, $\langle R_{g,\perp}^2 \rangle \propto (f\ell_p/k_B T)^{-2.5}$, seen for $f\ell_p/k_B T > 1$. However, we warn the reader to take this seriously: a closer look reveals a slight but systematic curvature, and a plot versus $f\ell_p/k_B T$ on a linear rather than a logarithmic scale reveals that this apparent power law is nothing but the onset of an exponential decay (Figs. 8c,d): indeed, already from the partition function, Eq. (62) we recognize that for large forces the chains will be stretched out almost completely like rigid rods, and the few remaining kinks are suppressed exponentially when $f\ell_p/k_B T \gg 1$.

For completeness, we show the corresponding simulation data for the relative extension $\langle X \rangle/L$ vs. $f\ell_p/k_B T$ in Fig. 9 (related more extensive data for other values of L and q_b can be found in Ref. [13]), and in Fig. 10 we present the corresponding data for the longitudinal component $\langle R_{g,\parallel}^2 \rangle/L^2$ of the gyration radius in the di-

rection of the force. While for very small forces one expects a nonzero plateau (unlike $\langle X \rangle/L$, which vanishes as $f \rightarrow 0$), corresponding to the gyration radius square component of an unstretched chain, for large f another plateau means that the chain has been stretched out fully to a rod of length L . In between these two plateaus, the Pincus blob behavior is seen rather clearly, for the flexible chains.

Fig. 11 now shows typical data for $S_\perp(q_\perp)$ vs. q_\perp and Fig. 12 the corresponding data for $S_\parallel(q_\parallel)$ vs. q_\parallel , focusing again on those selected values of q_b that were used already in Figs. 8-10. As expected from Eq. (47), the perpendicular structure factor is similar to the case without stretching force; the plateau at small q , where $S_\perp(q_\perp)$ deviates only very little from unity, gets more extended with increasing f , reflecting the decrease of $\langle R_{g,\perp}^2 \rangle$ with f (Fig. 8). This decrease, of course, is more pronounced for stiff chains than for flexible chains at the same value

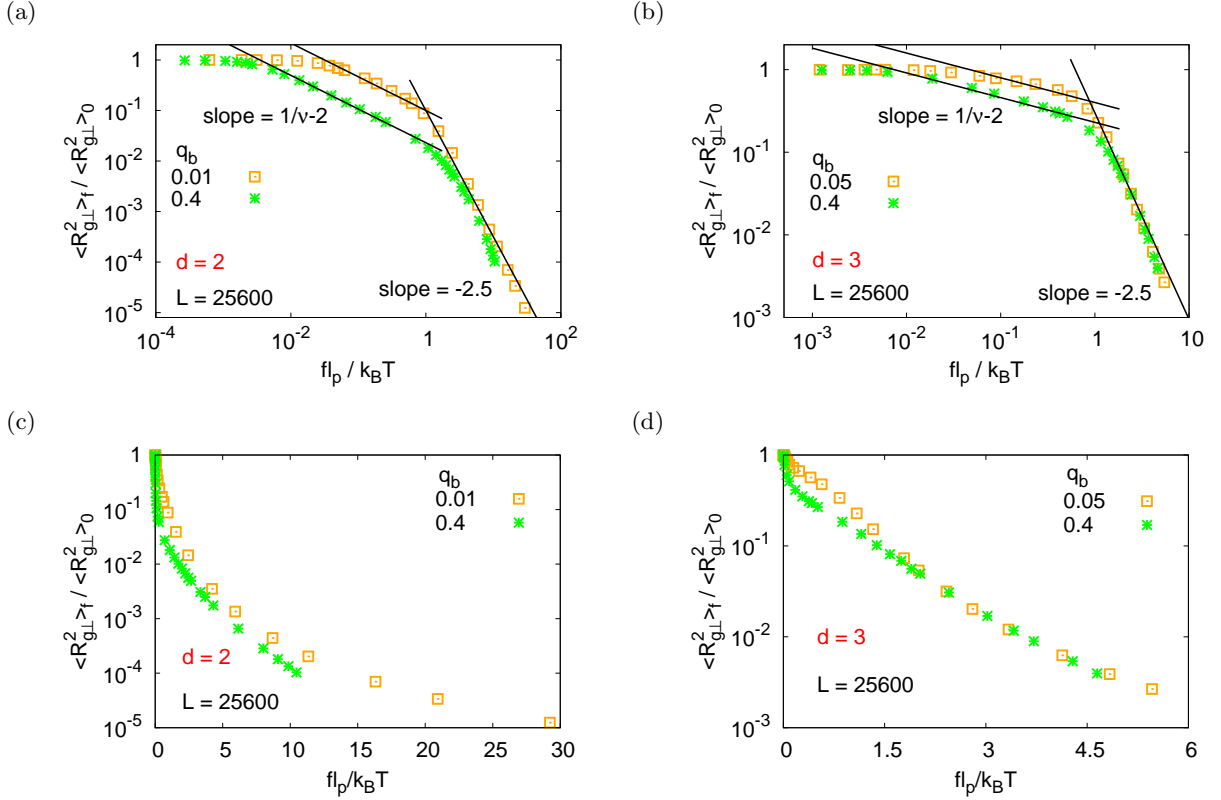


FIG. 8: Log-log plot of $\langle R_{g,\perp}^2 \rangle / \langle R_{g,\perp}^2 \rangle_0$ vs. $f\ell_p / k_B T$, for $d = 2$ (a) and for $d = 3$ (b), using $L = N\ell_b = 25600$ in both cases, for two choices of q_b . In parts (c,d) the same data as in (a,b) for large $f\ell_p / k_B T$ are replotted choosing a linear scale for $f\ell_p / k_B T$, to show that the behavior is compatible with an exponential decay in $d = 3$.

of f , since we have seen (see Fig. 8 and the discussions in Ref. [13]) that the proper control variable is not $f/k_B T$ but rather $f\ell_p / k_B T$. A further remarkable feature is the fact, that the power law-like decay of $S_\perp(q_\perp)$ with q_\perp , that for flexible chains can be observed until $S_\perp(q_\perp)$ has decayed up to $S_\perp(q_\perp) \approx 10^{-4}$ as $b < 1.5$, for stiff chains extends only to $S_\perp(q_\perp) \approx 10^{-3}$ in $d = 3$ and $S_\perp(q_\perp) \approx 10^{-2}$ in $d = 2$, respectively. As expected, the theory of Benoit et al. [40] which extended the description of scattering from Gaussian chains to elastic stretching deformations, can only be applied if $q_\perp \ell_p \ll 1$, and when $\langle R_{g,\perp}^2 \rangle$ exceeds ℓ_p^2 only by few orders of magnitudes, the applicability of Eq. (47) is correspondingly restricted. In fact, noting that, for $q_b = 0.05$, $\ell_p / \ell_b \approx 5.9$, we conclude that $b = 1.5$ means $f\ell_p / k_B T \approx 2.4$, and Fig. 8 shows that in this case indeed $\langle R_{g,\perp}^2 \rangle$ is about an order of magnitude smaller than for $f = 0$. Assuming that one can represent a stiff chain as a sequence of rods of length ℓ_p such that $n_p \ell_p = N\ell_b$, and stating in the spirit of Eq. (16) that at large q_\perp interference effects of different rods can be neglected, one would expect that for $q_\perp \ell_p \approx 1$ one obtains a scattering of the order of $S_\perp(q_\perp) \approx n_p^{-1}$, independent of q_\perp . This (admittedly rough) argument would qualitatively explain the systematic increase of the plateau $S(q)$ in Fig. 5 and $S_\perp(q_\perp)$ in Fig. 11 with increasing chain

stiffness.

Even more interesting is the behavior of $S_\parallel(q_\parallel)$, Fig. 12. The rapid increase of $\langle R_{g,\parallel}^2 \rangle$ with increasing stretching force has the consequence that $S_\parallel(q_\parallel)$ deviates from unity for smaller and smaller q_\parallel . While for small f just a shoulder develops, before (at large q_\parallel) the behavior is similar to that of $S_\perp(q_\perp)$, for large f pronounced oscillations develop. As pointed out already by Pierleoni et al. [44] for the case of fully flexible chains under stretch, this behavior can be attributed to the fact that the chain behaves like an elastically stretched string. We shall discuss this behavior in more detail below. Here we only note that the maxima of these oscillations decay according to a power law, which is similar to the power law of $S_\perp(q_\perp)$ in the intermediate range of q_\perp . The minima of $S_\parallel(q_\parallel)$, as well as $S_\parallel(q_\parallel)$ itself at larger values of q_\parallel where the oscillations of q_\parallel have decayed, show a slow further decrease with q_\parallel . While for very large $q_\parallel = q_\perp$ but not very strong stretching ($b < 1.5$) we have $S_\parallel(q_\parallel) = S_\perp(q_\perp)$, if the chains are flexible ($q_b = 1$, $q_b = 0.4$), this is not the case for stiff chains: $S_\parallel(q_\parallel) \ll S_\perp(q_\perp)$ for $q_\parallel = q_\perp$ then.

In order to understand these results more quantitatively, we first report $S_\perp(q_\perp)$ in form $q_\perp^2 S_\perp(q_\perp)$ versus q_\perp and compare to the Debye function, Eq. (47), but us-

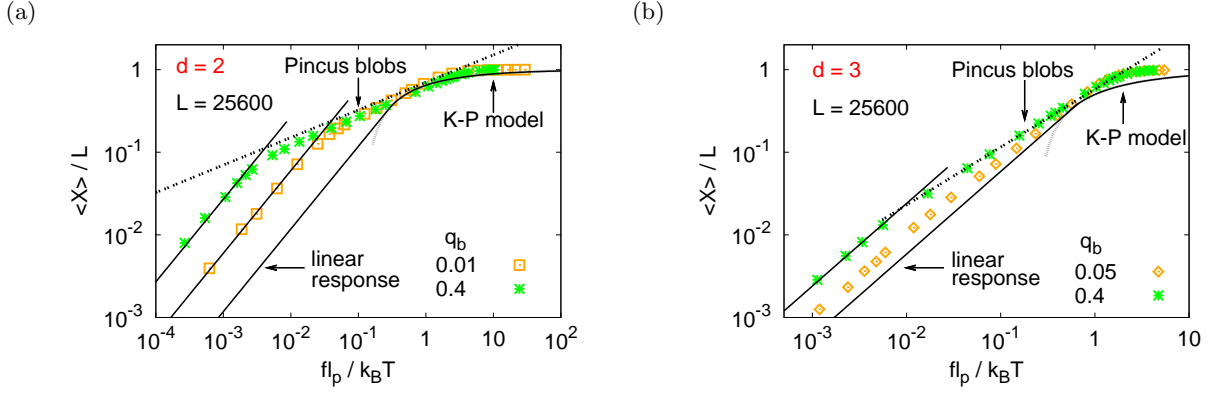


FIG. 9: Log-log plot of the relative extension $\langle X \rangle / L$ versus the scaled force $f \ell_p / k_B T$ for $L = 25600$ in $d = 2$ (a) and $d = 3$, for the same choices of q_b as shown in Fig. 8. The straight lines indicate the linear response regime and the Pincus-blob regime, respectively {Eq. (59)}. In neither case has the Kratky-Porod model (curves labeled as K-P-model, cf. Eqs. (54), (55)) a well-defined regime of validity (this is expected since for large $f \ell_p / k_B T$ the approach to saturation, $\langle X \rangle / L \rightarrow 1$, is exponentially fast rather than proportional to $(k_B T / f \ell_p)^{1/2}$, cf. Fig. 8).

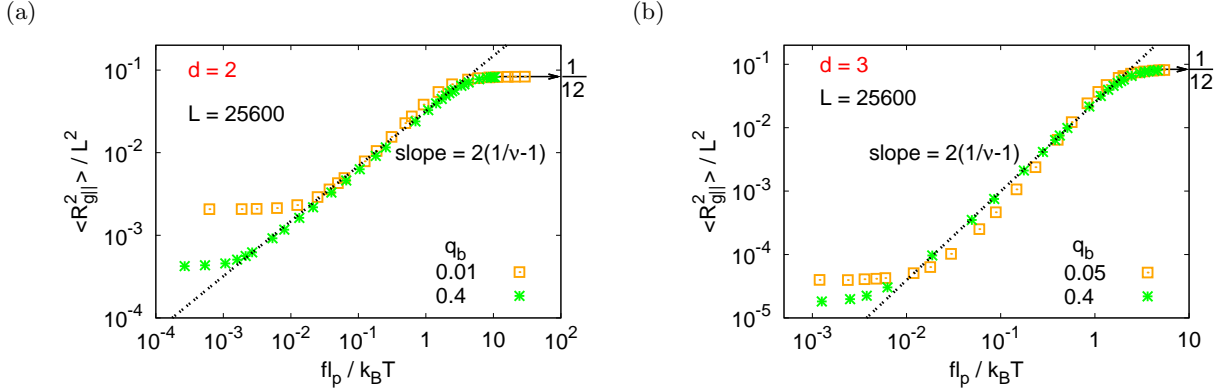


FIG. 10: Log-log plot of the parallel component $\langle R_{g,||}^2 \rangle / L^2$ vs. $f \ell_p / k_B T$, for the same parameters as in Figs. 8, 9. Straight lines indicate the Pincus blob regime. Part (a) refers to $d = 2$, part (b) to $d = 3$.

ing the value $\langle R_{g,\perp}^2 \rangle$ as observed in the simulation (rather than any theoretical prediction for it). Fig. 13 shows that the Debye function works surprisingly well: for $d = 3$ the slope $2 - 1/\nu$ indicating non-Gaussian behavior is seen for $q_b = 0.4$ only for weak stretching ($b = 1.001$ and 1.003), while for larger stretching forces a horizontal part in the plot $q_{\perp}^2 S_{\perp}(q)$ has developed. Also in $d = 2$ the excluded volume regime, where the slope $2 - 1/\nu$ is compatible with the data, is pronounced only for rather flexible chains (such as $q_b = 0.4$, Fig. 13c) while for stiff chains in $d = 2$ (such as $q_b = 0.01$) excluded volume effects show up in $S_{\perp}(q_{\perp})$ only for extremely weak stretching (such as $b = 1.0001$, i.e. $f/k_B T = 10^{-4}$). for stronger stretching of semiflexible chains in $d = 2$ the Debye function seems to describe the data for small q_{\perp} ($q_{\perp} \leq 10^{-2}$), but then a crossover to a behavior $S_{\perp}(q_{\perp}) \approx \text{const}$ and hence

$$q_{\perp}^2 S_{\perp}(q_{\perp}) \propto q_{\perp}^2 \text{ sets in.}$$

The behavior of $S_{||}(q_{||})$ when plotted in the form $q_{||}^2 S_{||}(q)$ vs. $q_{||}$ is particularly striking (Fig. 14). Again excluded volume effects (described in this representation by a slope $2 - 1/\nu$ again) are pronounced only for very small forces, while for somewhat larger forces (such as in $d = 3$ for $b \geq 1.070$ for $q_b = 0.4$ and for $b \geq 1.015$ for $q_b = 0.05$, and in $d = 2$ for $b \geq 1.015$ for $q_b = 0.4$ and for $b \geq 1.005$ for $q_b = 0.01$), the oscillatory behavior of the structure factor, as described by the Debye function with complex $X_{||}$ {Eq. (46)}, sets in. In order to interpret this behavior in more detail, we write $X_{||} = a + ic$, where $a = q_{||}^2 (\langle X^2 \rangle - \langle X \rangle^2) / 2$ and $c = q_{||} \langle X \rangle$, to rewrite Eq. (47) as follows

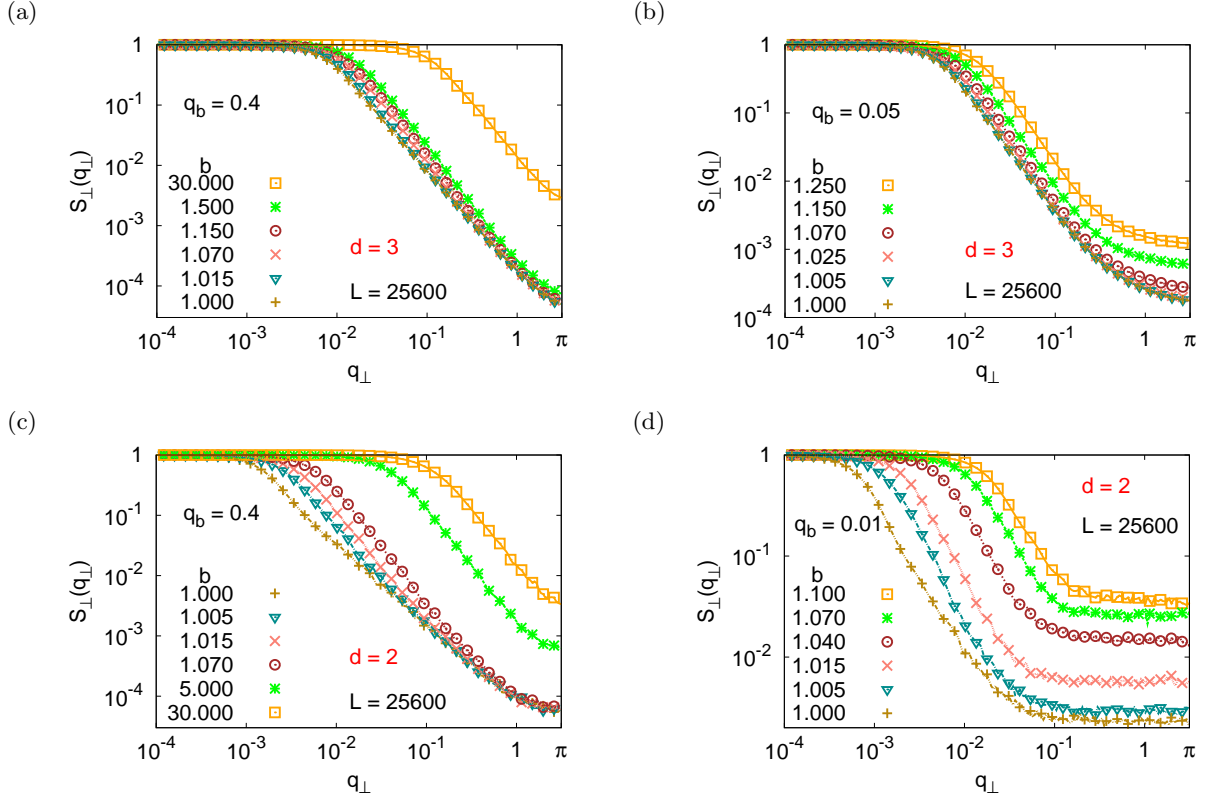


FIG. 11: Log-log plot of the structure factor $S_{\perp}(q_{\perp})$ vs. q_{\perp} for $d = 3$ and two choices of the stiffness parameter q_b , $q_b = 0.4$ (a) and $q_b = 0.05$ (b), and also for $d = 2$ and two choices of q_b , namely $q_b = 0.4$ (c) and $q_b = 0.01$. In each case several choices of $b = \exp(f/k_B T)$ are included, as indicated. Chain length is $L = 25600$ throughout.

$$S_{||}(q_{||}) = 2 \frac{\exp(-a) [(a^2 - c^2) \cos c - 2ac \sin c] + a^3 + ac^2 + c^2 - a^2}{(a^2 + c^2)^2} \quad (63)$$

We recognize that there are two rather distinct parts, an exponentially damped oscillatory part and a “background part” which survives when the oscillatory part has died out. For $a \gg 1$ this background part can be written as (note that for large stretching there is a regime where $a^2 \ll c^2$)

$$S_{||}(q_{||}) \approx \frac{2a}{c^2} = \frac{\langle X^2 \rangle}{\langle X \rangle^2} - 1 \quad (64)$$

In the regime where the oscillations have died out again and there is hence a flat part of $S_{||}(q_{||})$, independent of $q_{||}$ again, the structure factor hence measures the relative fluctuation in the length of the strongly stretched polymer.

Let us now consider the oscillatory part of Eq. (63). Since we are in a regime where $a^2 \ll c^2$, the maxima are reached when $\cos c = -1$ and in the regime where $a \ll 1$

and hence $\exp(-a) \approx 1$ we hence have

$$S_{||}^{\max}(q_{||}) \approx \frac{4}{c^2} = \frac{4}{q_{||}^2 \langle X \rangle^2}, \quad (65)$$

$$q_{||} \langle X \rangle = (2m + 1)\pi, \quad m = 0, 1, \dots$$

and hence $q_{||}^2 S_{||}^{\max} \approx \text{const}$, as observed from the full calculation of Eq. (63), and the simulation.

When we compare these results to the scattering from the rigid rods, however, Eq. (30) predicts maxima that are undamped and minima that are strictly zero, so for increasing $q_{||}$ the oscillations continue forever. However, this is a result for a rod that has a strictly fixed length L_{rod} , while the polymer under strong stretch (with extension $\langle X \rangle$ such that $1 - \langle X \rangle / L \ll 1$) still is only similar to a rod of fluctuating length, and this in fact is borne out by the structure factor at large q {Eq. (64)}.

In any case the success of the Debye function, Eqs. (46), (63) for the description of the scattering from

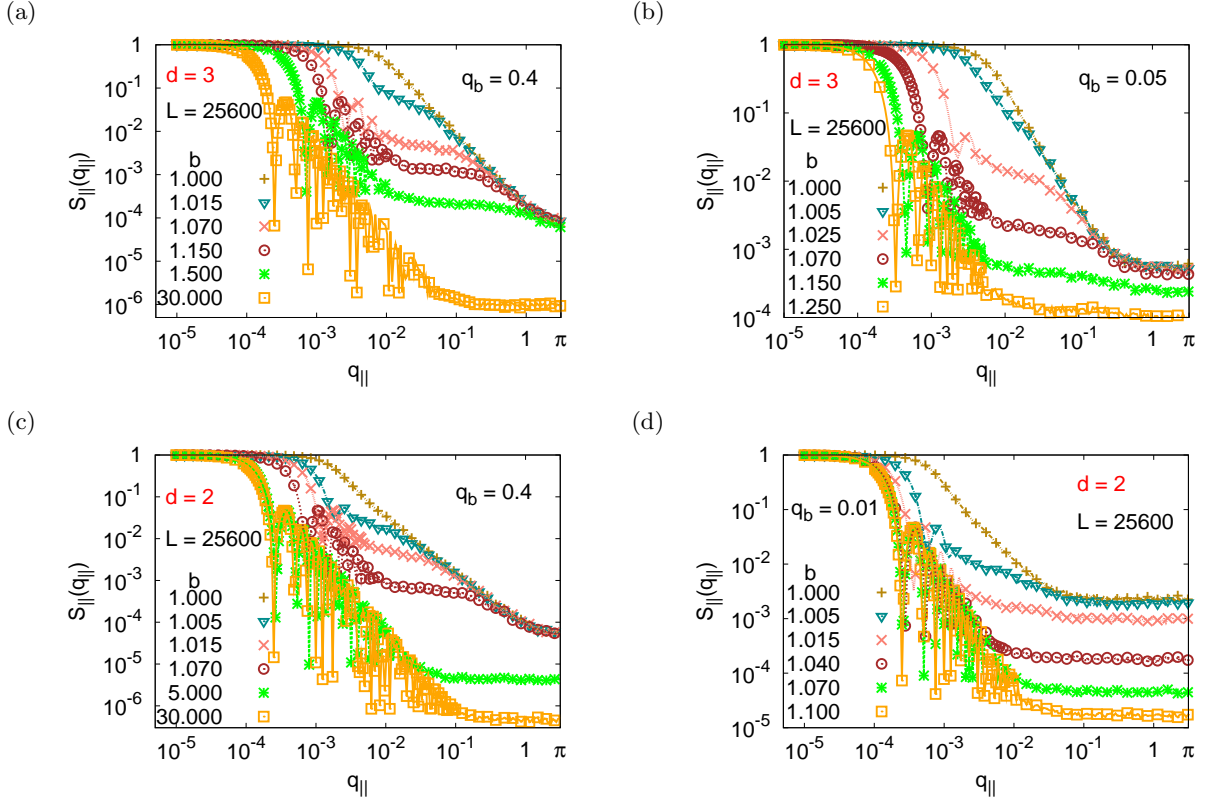


FIG. 12: Log-log plot of the structure factor $S_{||}(q_{||})$ vs. $q_{||}$ for $d = 3$ and two choices of the stiffness parameter q_b , $q_b = 0.4$ (a) and $q_b = 0.05$ (b), and also for $d = 2$ and two choices of q_b , namely $q_b = 0.4$ (c) and $q_b = 0.01$ (d). In each case several choices of $b = \exp(f/k_B T)$ are included. Chain length is $L = 25600$ throughout.

strongly stretched chains in both $d = 2$ and $d = 3$ dimensions is very remarkable, since it is derived from Gaussian chain statistics [40], and we have seen that in $d = 2$ in the absence of stretching forces Gaussian chain statistics does not work in $d = 2$, irrespective of chain stiffness.

At the end of this section, we emphasize that the examples given for the success of the Debye function for stretched chains, as derived by Benoit et al. [40], are not accidental, but this behavior is typical for a wide range of chain stiffnesses. As an example, we show further data for $S_{\perp}(q_{\perp})$ in both $d = 2$ and $d = 3$ and various other choices of the stiffness parameter q_b in Figs. 15, 16. Whenever the plots indicate a well-defined plateau, one can extract an estimate of $\langle R_{g,\perp}^2 \rangle$ from it (note that the actual values of $\langle R_{g,\perp}^2 \rangle$ that were independently estimated were used to predict the Debye functions as shown in Figs. 15, 16.). As has been shown already in Fig. 8, the radii $\langle R_{g,\perp}^2 \rangle$ do have a broad regime of forces $f/k_B T$ where excluded volume effects (“Pincus blob” - behavior) prevail, so the success of the Debye function must not be over-emphasized, it does not mean that the chain conformation follow Gaussian statistics.

VI. CONCLUSIONS

In this paper we have presented a comparative simulation study of the single-chain structure factor $S(q)$ for variable stiffness of the macromolecules in both $d = 2$ and $d = 3$ dimensions, both for coils in equilibrium in dilute solution under good solvent conditions, and for polymers under the influence of a stretching force. Characteristic linear dimensions of the macromolecules that are needed in the theoretical interpretation of $S(q)$, have in our Monte Carlo simulation always been estimated directly and hence independently, such as the mean square gyration radius $\langle R_g^2 \rangle$ and the persistence length ℓ_p . In the presence of stretching forces, the extension $\langle X \rangle$ in the direction of the force (as well as fluctuations $\langle X^2 \rangle - \langle X \rangle^2$, and components of the gyration radius $\langle R_{g,\perp}^2 \rangle$ and $\langle R_{g,\parallel}^2 \rangle$) have been obtained as well. Of course, as usual the simulations are performed for the strictly monodisperse case, the number of bonds N and hence also the contour length $L = N\ell_b$ of the chain molecules are known input parameters of the simulation. In this respect, a more definite interpretation of the outcome of the simulations can be expected, than would be expected for corresponding experiments (where polydispersity is a problem, and often the average contour length is not a priori known but

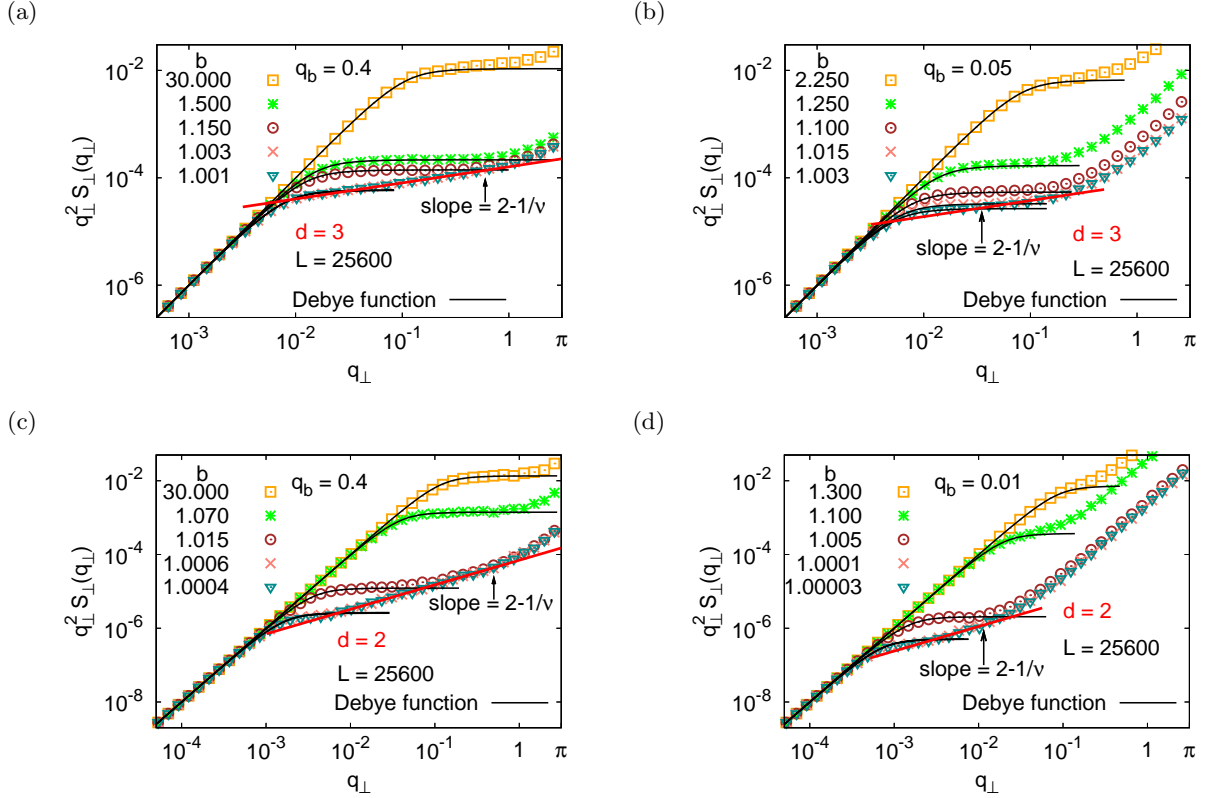


FIG. 13: Log-log plot of $q_{\perp}^2 S_{\perp}(q_{\perp})$ vs. q_{\perp} for $d = 3$ and two choices of the stiffness parameter q_b , $q_b = 0.4$ (a) and $q_b = 0.05$ (b), and also for $d = 2$ and two choices of q_b , namely $q_b = 0.4$ (c) and $q_b = 0.01$ (d). The curves are the Debye function, Eq. (47) with $X_{\perp} = \frac{3}{2}q_{\perp}^2 \langle R_{g,\perp}^2 \rangle$ in $d = 3$, and $X_{\perp} = 3q_{\perp}^2 \langle R_{g,\perp}^2 \rangle$ in $d = 2$. In each case several choices of $b = \exp(f/k_B T)$ are included. Chain length is $L = 25600$ throughout.

must also be extracted from fitting suitable experimental data). Of course, the drawback of our Monte Carlo simulations on a lattice is the highly idealized character of such coarse-grained model as used here, the self-avoiding walk with additional energy penalty for making kinks. Nevertheless, the comparison between our simulation results for the mean square gyration radius versus the number of “Kuhn segments” n_K with corresponding experimental data (Fig. 1) is very encouraging: one not only notes a striking similarity between simulation and experiment, but we stress that also the same range of dimensionless variables (n_K and $\langle R_g^2 \rangle / (2\ell_p)^2$) is accessible. The simulation has the bonus that directly single-chain properties are accessible (no extrapolation as a function of the concentration c of the solution towards $c \rightarrow 0$ is required and by changing the energy parameter $\epsilon_b/k_B T$, that describes the cost of making a kink along the walk, in units of the thermal energy, the stiffness is easily controlled. In experiment, stiffness can only be widely varied by combining data for polymers with different chemical structure.

From our data we have confirmed a conclusion drawn already from our previous study of mean square end-to-end distances, namely that in $d = 2$ a direct crossover

occurs from rod-like behavior to self-avoiding walks, with a scaling $\langle R_g^2 \rangle \propto \ell_p^{1/2} L^{3/2}$, without the existence of any intermediate regime with Gaussian behavior (Fig. 3). In $d = 3$, however, such an intermediate regime has been found, Fig. 2, for $1 \ll n_K \ll n_K^* \propto (\ell_p/D)^{\zeta}$, where D is the local chain diameter and the exponent ζ is in the range $1.5 \leq \zeta \leq 2$. Thus, there is no universal value n_K^* where excluded volume effects set in, but rather $n_K^* \rightarrow \infty$ for $\ell_p/D \rightarrow \infty$.

In the equilibrium structure factor $S(q)$, in the absence of stretching forces, correspondingly several regimes can be distinguished. For small enough q , the standard Guinier behavior always occurs, which contains the information on $\langle R_g^2 \rangle$, of course. For $d = 2$, one then always has the excluded volume regime (for long enough chains), $S(q) \propto q^{-4/3}$, and possibly (for rather stiff chains) a crossover to rod-like behavior ($S(q) \propto q^{-1}$) sets in gradually. A Gaussian behavior $S(q) \propto q^{-2}$ is never seen, unlike the case $d = 3$, where this behavior does become visible for very stiff chains (before for still larger q the rod-like behavior starts). The excluded volume power law, $S(q) \propto q^{-1/\nu}$ with $\nu \approx 0.588$, is only visible for not very stiff chains (if chain lengths $L \leq 25600$ are analyzed, as done here: if $L \rightarrow \infty$, this power law would emerge for

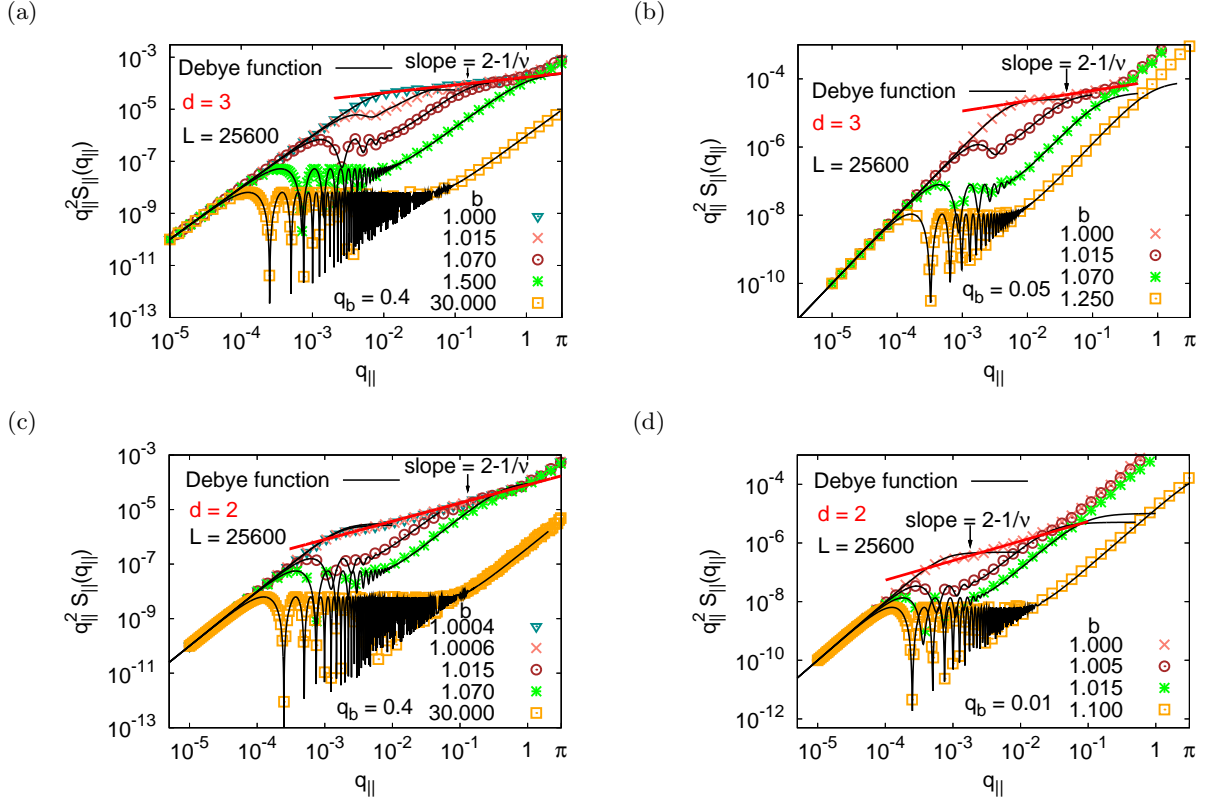


FIG. 14: Log-log plot of $q_{\parallel}^2 S_{\parallel}(q_{\parallel})$ vs. q_{\parallel} for $d = 3$ and two choices of the stiffness parameter q_b , namely $q_b = 0.4$ (a) and $q_b = 0.05$ (b), and also for $d = 2$ and two choices of $q_b = 0.4$ (c) and $q_b = 0.01$ (d). The curves are the Debye function, Eq. (63) with complex $X_{\parallel} = q_{\parallel}^2(\langle X^2 \rangle - \langle X \rangle^2)/2 + iq_{\parallel} \langle X \rangle$, and the straight line shows the excluded volume power law (slope = $2 - 1/\nu$). In each case several choices of $b = \exp(f/k_B T)$ are included. Chain length is $L = 25600$ throughout.

any finite value of the persistence length, of course). This pattern of behavior (Fig. 4), of course, could have been a priori expected, but we are also able to show via Kratky plots ($qLS(q)$ vs. qL) that for semiflexible chains in $d = 3$ the expressions derived by Kholodenko and by Stepanow provide a quantitatively accurate description. It is found that for large q this quantity $qLS(q)$ settles down at π , unlike the behavior predicted for flexible chains (the Debye function predicts $qLS(q) \propto q^{-1}$ for large q). However, the onset of the plateau occurs gradually in the decade $1 < q\ell_p < 10$; thus the onset of the plateau allows an estimation of ℓ_p only somewhat roughly. The peak position of the Kratky plot (Figs. 5,6) reflects the theoretically expected scaling of the gyration radius with L and ℓ_p , even though in the Kratky plot (Fig. 5) direct evidence for excluded volume effects seem to be minor.

Des Cloizeaux [23] derived from the Kratky-Porod model that for $L \rightarrow \infty$ one should have $LqS(q) = \pi + \text{const}(q\ell_p)^{-1}$, with the constant being predicted to be $2/3$ {Eq. (1)}. Unfortunately, this result is at variance with our numerical results (Fig. 7). The reason for this problem is still not clear.

Turning to the behavior of chains under the influence of stretching forces, we have shown that for weak forces,

where linear response holds, excluded volume effects invalidate the Kratky-Porod model completely in $d = 2$ dimensions, and one typically observes a broad range of forces where the extension versus force relation is a power law, and also $\langle R_{g\perp}^2 \rangle, \langle X^2 \rangle - \langle X \rangle^2$ are found to scale like $(f\ell_p/k_B T)^{1/\nu-2}$ in this ‘‘Pincus blob’’ regime. In $d = 3$, dimensions, however, a Pincus blob regime also exists, but its observability also is restricted. For large $k_B T/f$, however, the (continuum) Kratky-Porod descriptions is not valid for our discrete lattice model either: it is found that then $\langle R_{g\perp}^2 \rangle$ and $\langle X^2 \rangle - \langle X \rangle^2$ decrease like $\exp(-f/k_B T)$ for $f/k_B T \gg 1$.

Although the excluded volume effects show up rather clearly in the chain extensions and gyration radii components, it turns out that Benoit’s extension of the Debye formula to stretched chains [40] is a surprisingly accurate description of both the transverse ($S_{\perp}(q_{\perp})$) and parallel parts ($S_{\parallel}(q_{\parallel})$) of the structure factor. The oscillatory behavior of $S_{\parallel}(q_{\parallel})$ for strongly stretched chains shows that their conformations resemble a string of elastically coupled particles. Thus, if measurable, the structure factor of stretched chains would add valuable details to the picture of their conformations.

As we have emphasized in our paper, the statistical

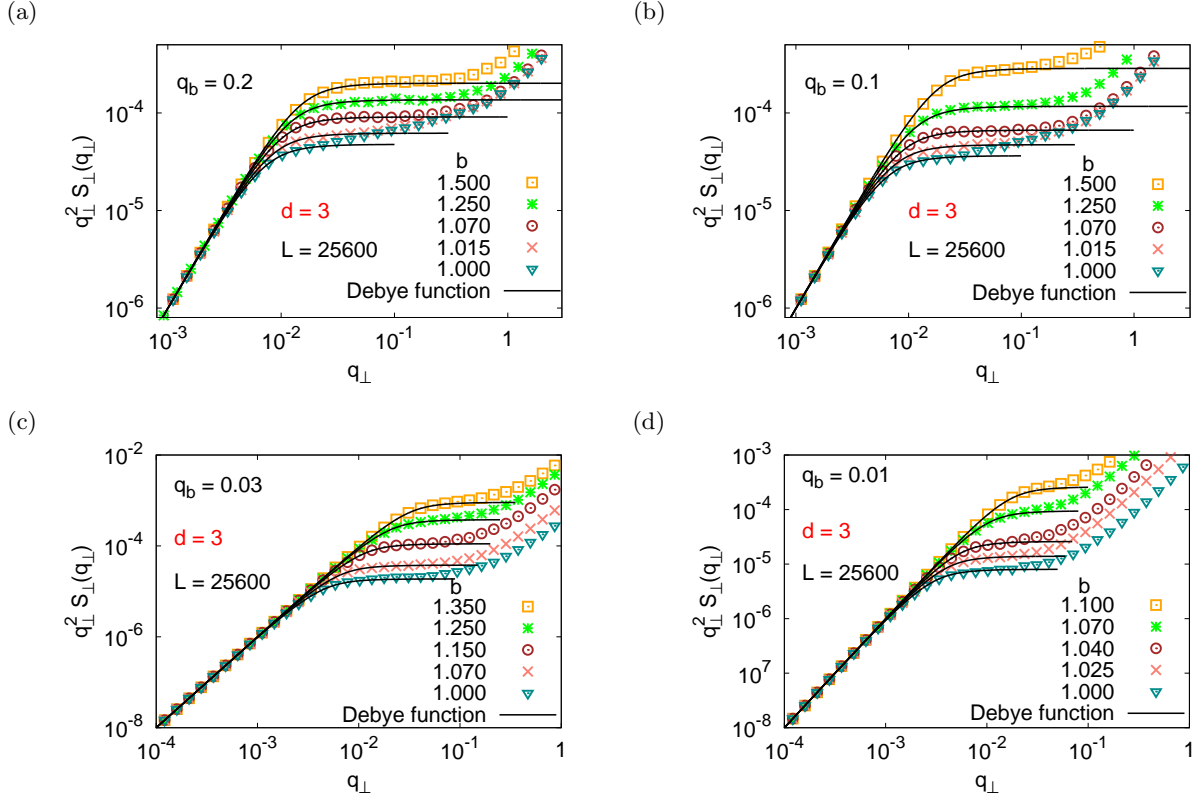


FIG. 15: Log-log plot of $q_{\perp}^2 S_{\perp}(q_{\perp})$ vs. q_{\perp} in $d = 3$ dimensions for $q_b = 0.2$ (a), 0.1 (b), 0.03 (c) and 0.01 (d), for several choices of the force parameter $b = \exp(f/k_B T)$, as indicated. The curves are the Debye function, Eq. (47) with $X_{\perp} = \frac{3}{2} q_{\perp}^2 \langle R_{g,\perp}^2 \rangle$. When the data settle down at a horizontal plateau, it yields an estimate of $4/(3\langle R_{g,\perp}^2 \rangle)$.

mechanics of semiflexible polymers has been a longstanding and controversial problem of polymer science. The subject is of great relevance for biopolymers, but also of broad interest in material science. We expect that the present study will be useful both for the interpretation of experiments and stimulate further theoretical studies, such as of the interplay between solvent quality and chain stiffness.

Acknowledgments

We are grateful to the Deutsche Forschungsgemeinschaft (DFG) for support under grant No SFB 625/A3, and to the John von Neumann Institute for Computing (NIC Jülich) for a generous grant of computer time. We are particularly indebted to S. Stepanow for his help with the explicit calculation of his exact formula for the structure factor of the Kratky-Porod model. We are also indebted to Hyuk Yu for pointing out Ref. [12] to us, and to C. Pierleoni for drawing our attention to Ref. [44]. H.-P.

Hsu thanks K. Ch. Daoulas for stimulating discussions.

Appendix A: Scattering function of random walk chains under constant pulling force

The paper by Benoit et al. [40] uses the distribution function of the end-to-end vector of a Gaussian chain of $|i - j|$ repeat units for the calculation of the single chain scattering function. The result is the well-known Debye function.

Following an idea from Doi's book [74] one can derive the diffusion equation yielding the end-to-end vector distribution in the following way. Assume a step-wise Markov growth of the chain

$$P(\vec{R}, N) = \sum_i P(\vec{R} - \vec{l}_i, N - 1) p(\vec{l}_i). \quad (\text{A1})$$

The sum over “i” goes over an isotropic bond vector set, i.e., both \vec{l}_i and $-\vec{l}_i$ are members of the set.

Expanding the right side to first order in N and to second order in \vec{R} yields

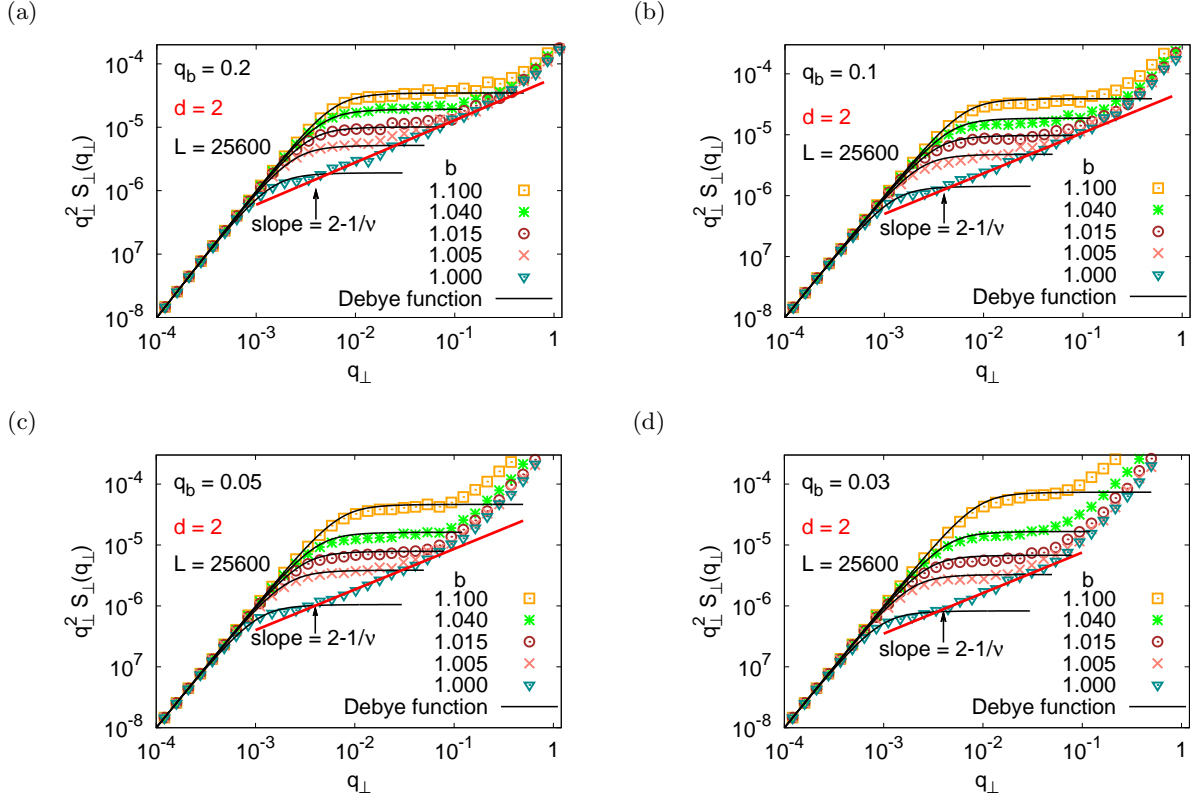


FIG. 16: Log-log plot of $q_{\perp}^2 S_{\perp}(q_{\perp})$ vs. q_{\perp} in $d = 2$ dimensions for $q_b = 0.2$ (a), 0.1 (b), 0.05 (c) and 0.03 (d), for several choices of the force parameter $b = \exp(f/k_B T)$, as indicated. The curves are the Debye function, Eq. (47) with $X_{\perp} = 3q_{\perp}^2 \langle R_{g,\perp}^2 \rangle$, and the straight line shows the excluded volume power law (slope = $2 - 1/\nu$). From the Debye plateau $2/(3\langle R_{g,\perp}^2 \rangle)$ can be extracted.

$$P(\vec{R} - \vec{l}_i, N - 1) = P(\vec{R}, N) - \frac{\partial P}{\partial N} - \sum_{\alpha=1}^3 \frac{\partial P}{\partial R_{\alpha}} l_{i,\alpha} + \frac{1}{2} \sum_{\alpha=1}^3 \sum_{\beta=1}^3 \frac{\partial^2 P}{\partial R_{\alpha} \partial R_{\beta}} l_{i,\alpha} l_{i,\beta} + \dots \quad (\text{A2})$$

Averaging the derivatives with respect to R_{α} with a symmetric bond probability $p(\vec{l}_i)$ (in the simplest case this is just one over the number of bonds) gives zero for the first derivative and $\delta_{\alpha\beta} l^2/3$ for the second term, resulting in the diffusion equation

$$\frac{\partial P}{\partial N} = \frac{l^2}{6} \nabla^2 P \quad (\text{A3})$$

Solving this for a bulk chain gives the well known result for the end-to-end vector distribution

$$P(\vec{R}, N) = (2\pi N l^2/3)^{-3/2} \exp\left(-\frac{3R^2}{2N l^2}\right), \quad (\text{A4})$$

The Debye function can then be derived by averaging with this probability, as is done in the Benoit et al. paper.

The derivation above is useful as a starting point for a calculation of the scattering function for a chain that

is pulled. In this case the bond probabilities are not symmetric. For our model we have

$$p_0 = \frac{b}{b^2 + 4b + 1} \quad (\text{A5})$$

$$p_+ = \frac{b^2}{b^2 + 4b + 1}$$

$$p_- = \frac{1}{b^2 + 4b + 1} \quad (\text{A6})$$

for moves perpendicular to the pulling direction, in $+X$ direction and in $-X$ direction, respectively, where $b = \exp(fl/k_B T)$ with $l = 1$ is used as in the main text. When we now perform the expansion of Eq. (A2) and perform the average over the bond probabilities we obtain

$$\frac{\partial P}{\partial N} = -(p_+ - p_-)l \frac{\partial P}{\partial X} + p_0 l^2 \left(\frac{\partial^2 P}{\partial Y^2} + \frac{\partial^2 P}{\partial Z^2} \right) + \frac{p_+ + p_-}{2} l^2 \frac{\partial^2 P}{\partial X^2} \quad (\text{A7})$$

For $p_+ = p_- = p_0$ this reduces to the normal diffusion equation. This equation has to be solved with the boundary conditions

$$\begin{aligned} P(\vec{R}, 0) &= \delta(\vec{R}) \\ P(\vec{R}, N) &\rightarrow 0 \quad \text{for} \quad R \rightarrow \infty \end{aligned} \quad (\text{A8})$$

Let us define $D_\perp = 2p_0 l^2$, $D_\parallel = (p_+ + p_-)l^2$, and $v = (p_+ - p_-)l$, so we have

$$\frac{\partial P}{\partial N} = -v \frac{\partial P}{\partial X} + \frac{1}{2} D_\perp \left(\frac{\partial^2 P}{\partial Y^2} + \frac{\partial^2 P}{\partial Z^2} \right) + \frac{1}{2} D_\parallel \frac{\partial^2 P}{\partial X^2}. \quad (\text{A9})$$

These are three diffusion processes in the three Cartesian directions, X is parallel to the force, Y and Z are perpendicular. The solutions for the perpendicular directions are the same as for the force-free case. For the parallel direction we have an altered diffusion coefficient and a drift part to the process, i.e., a Gaussian diffusion around a deterministic drift. The complete solution to Eq. (A9) is therefore given by

$$P(X, Y, Z, N) = \frac{1}{2\pi N D_\perp} \frac{1}{\sqrt{2\pi N D_\parallel}} e^{-\frac{Y^2 + Z^2}{2N D_\perp}} e^{-\frac{(x-vN)^2}{2N D_\parallel}}. \quad (\text{A10})$$

For $p_0 = p_+ = p_- = 1/6$ we obtain back the force free solution. To calculate the scattering function we follow the procedure employed in the calculation of the Debye function in the force free case.

$$S(\vec{q}) = \frac{1}{N^2} \sum_{i,j} \langle e^{i\vec{q} \cdot \vec{r}_{ij}} \rangle \quad (\text{A11})$$

can be calculated when we assume a continuous chain model (i.e. only look at distances much larger than the lattice constant) so that the distribution for the \vec{r}_{ij} is given by the Gaussian distribution we just calculated.

$$S(\vec{q}) = \frac{1}{N^2} \sum_{i,j} \int d^3 \vec{r}_{ij} P(\vec{r}_{ij}, |i-j|) e^{i\vec{q} \cdot \vec{r}_{ij}} \quad (\text{A12})$$

where we have $P(\vec{r}_{ij}, |i-j|) = P_Y(Y, |i-j|) P_Z(Z, |i-j|) P_X(X, |i-j|)$ and P_Y and P_Z have the same functional form and all P_i are normalized to one individually.

Scattering in the perpendicular direction

$$\begin{aligned} S(\vec{q}_\perp) &= \frac{1}{N^2} \sum_{i,j} \int dY \int dZ \\ &P_Y(Y, |i-j|) P_Z(Z, |i-j|) e^{i\vec{q}_\perp \cdot \vec{r}_{ij}} \end{aligned} \quad (\text{A13})$$

where $\rho_{ij} = Y\hat{e}_Y + Z\hat{e}_Z$. So we have to evaluate

$$\begin{aligned} S(q_\perp) &= \frac{1}{N^2} \sum_{i,j} \int dY \frac{1}{\sqrt{2\pi |i-j| D_\perp}} e^{-\frac{Y^2}{2|i-j| D_\perp}} e^{iq_Y Y} \\ &\int dZ \frac{1}{\sqrt{2\pi |i-j| D_\perp}} e^{-\frac{Z^2}{2|i-j| D_\perp}} e^{iq_Z Z} \end{aligned} \quad (\text{A14})$$

resulting in

$$S(q_\perp) = \frac{1}{N^2} \sum_{i,j} e^{-\frac{q_\perp^2 |i-j| D_\perp}{2}} \quad (\text{A15})$$

This is evaluated by a continuum approximation for the two sums, $\sum_i \rightarrow \int_0^N du$ and $\sum_j \rightarrow \int_0^N dv$ which finally yields:

$$S(q_\perp) = \frac{4}{N q_\perp^2 D_\perp} + \frac{8}{N^2 q_\perp^4 D_\perp^2} \left(e^{-\frac{q_\perp^2 D_\perp N}{2}} - 1 \right). \quad (\text{A16})$$

Scattering in the parallel direction

$$S(q_\parallel) = \frac{1}{N^2} \sum_{i,j} \int dX \frac{1}{\sqrt{2\pi |i-j| D_\parallel}} e^{-\frac{(x-v|i-j|)^2}{2|i-j| D_\parallel}} e^{iq_\parallel X} \quad (\text{A17})$$

which now results in

$$S(q_\parallel) = \frac{1}{N^2} \sum_{i,j} e^{-\frac{q_\parallel^2 |i-j| D_\parallel}{2}} \cos(q_\parallel v |i-j|). \quad (\text{A18})$$

Performing the final calculation again in the continuum approximation gives

$$\begin{aligned} S(q_\parallel) &= \frac{4}{N} \frac{D_\parallel q_\parallel^2}{q_\parallel^4 D_\parallel^2 + 4v^2 q_\parallel^2} \\ &+ \frac{8}{N^2} \frac{q_\parallel^4 D_\parallel^2 - 4v^2 q_\parallel^2}{(q_\parallel^4 D_\parallel^2 + 4v^2 q_\parallel^2)^2} \left(e^{-\frac{q_\parallel^2 D_\parallel N}{2}} \cos(Nv q_\parallel) - 1 \right) \\ &- \frac{32}{N^2} \frac{q_\parallel^3 D_\parallel v}{(q_\parallel^4 D_\parallel^2 + 4v^2 q_\parallel^2)^2} e^{-\frac{q_\parallel^2 D_\parallel N}{2}} \sin(Nv q_\parallel) \end{aligned} \quad (\text{A19})$$

This result determines our scattering functions with parameters depending on the applied force f , so these equations contain no free parameters. Note that both functions reduce to the Debye function for the force free isotropic case ($v = 0$, $D_\perp = D_\parallel = l^2/3$) as it should be, because the scattering function does not depend on the direction of the scattering vector in this case.

For fitting purposes it might yield better results to replace some of the quantities by average values determined in the simulation. For the Y and the Z components simple Gaussian statistics holds

$$\langle Y \rangle = \langle Z \rangle = 0 \quad (\text{A20})$$

$$\langle Y^2 \rangle = \langle Z^2 \rangle = ND_{\perp} \quad (\text{A21})$$

$$\langle R_{g,Y}^2 \rangle = \langle R_{g,Z}^2 \rangle = \frac{ND_{\perp}}{6} \quad (\text{A22})$$

but in the force direction we can calculate from Eq. (A10) for the moments of the end-to-end distance

$$\langle X \rangle = Nv \quad (\text{A23})$$

$$\langle X^2 \rangle = N^2v^2 + ND_{\parallel} \quad (\text{A24})$$

$$\langle \Delta X^2 \rangle = ND_{\parallel} \quad (\text{A25})$$

$$\langle R_{g,X}^2 \rangle = \frac{ND_{\parallel}}{6} + \frac{D_{\parallel}N^2v^2}{12}. \quad (\text{A26})$$

When we now rewrite the scattering functions in terms of moments of the end-to-end vector or gyration tensor, we obtain

$$S(q_{\perp}) = \frac{4}{3q_{\perp}^2 \langle R_{g,\perp}^2 \rangle} + \frac{8}{[3q_{\perp}^2 \langle R_{g,\perp}^2 \rangle]^2} \left(e^{-\frac{3q_{\perp}^2 \langle R_{g,\perp}^2 \rangle}{2}} - 1 \right). \quad (\text{A27})$$

This is the Debye function with the appropriate prefactors, because for $\langle R_{g,\perp}^2 \rangle = 2/3 \langle R_g^2 \rangle$ it reduces to the standard function, Eq. (22). For the scattering parallel to the pulling direction we can write

$$S(q_{\parallel}) = 4 \frac{q_{\parallel} \langle \Delta X^2 \rangle}{q_{\parallel}^4 \langle \Delta X^2 \rangle^2 + 4q_{\parallel}^2 \langle X \rangle^2} + 8 \frac{q_{\parallel}^4 \langle \Delta X^2 \rangle^2 - 4q_{\parallel}^2 \langle X \rangle^2}{(q_{\parallel}^4 \langle \Delta X^2 \rangle^2 + 4q_{\parallel}^2 \langle X \rangle^2)^2} \left(e^{-\frac{q_{\parallel}^2 \langle \Delta X^2 \rangle}{2}} \cos(q_{\parallel} \langle X \rangle) - 1 \right) - 32 \frac{q_{\parallel}^3 \langle \Delta X^2 \rangle \langle X \rangle}{(q_{\parallel}^4 \langle \Delta X^2 \rangle^2 + 4q_{\parallel}^2 \langle X \rangle^2)^2} e^{-\frac{q_{\parallel}^2 \langle \Delta X^2 \rangle}{2}} \sin(q_{\parallel} \langle X \rangle). \quad (\text{A28})$$

This gives the same formula as Eq. (63) when X_{\parallel} in Eq. (46) is written by $X_{\parallel} = a + ic$ with $a = q_{\parallel}^2 \langle \Delta X^2 \rangle / 2$, and $c = q_{\parallel} \langle X \rangle$. For $\langle X \rangle = 0$ and $\langle \Delta X^2 \rangle = \langle X^2 \rangle = 6 \langle R_{g,X}^2 \rangle = 2 \langle R_g^2 \rangle$ this again reduces to the Debye function, Eq. (22).

Scattering in $d = 2$

Both scattering functions as calculated in Eqs. (A16) and (A19) remain formally unchanged. However, the probabilities for the single steps change to

$$\begin{aligned} p_0 &= \frac{b}{b^2 + 2b + 1} \\ p_+ &= \frac{b^2}{b^2 + 2b + 1} \\ p_- &= \frac{1}{b^2 + 2b + 1} \end{aligned} \quad (\text{A29})$$

The parallel and perpendicular diffusion coefficients as well as the drift velocity still have the same functional dependence on these probabilities. However, introducing the chain extensions into Eqs. (A16) and (A19) for $d = 2$ changes the prediction Eq. (A28) for the perpendicular scattering to

$$S(q_{\perp}) = \frac{2}{3q_{\perp}^2 \langle R_{g,\perp}^2 \rangle} + \frac{2}{(3q_{\perp}^2 \langle R_{g,\perp}^2 \rangle)^2} \left(e^{-3q_{\perp}^2 \langle R_{g,\perp}^2 \rangle} - 1 \right), \quad (\text{A30})$$

whereas it leaves Eq. (A28) unchanged. Taking $X_{\perp} = 3q_{\perp}^2 \langle R_{g,\perp}^2 \rangle$, the expression of Eq. (A30) has the same formula as Eq. (47).

-
- [1] P. G. de Gennes, *Scaling Concepts in Polymer Physics* (Cornell University Press, Ithaca, NY, 1979).
 - [2] J. Des Cloizeaux and G. Jannink, *Polymers in Solution: Their Modeling and Structure* (Clarendon Press, Oxford, UK, 1990).
 - [3] L. Schäfer, *Excluded Volume Effects in Polymer Solutions as Explained by the Renormalization Group* (Springer, Berlin, 1999).
 - [4] J. S. Higgins and H. C. Benoit, *Polymers and Neutron Scattering* (Clarendon Press, Oxford, 1994).
 - [5] P. J. Flory, *Principles of Polymer Chemistry* (Cornell University Press, NY, 1953).
 - [6] M. Rubinstein and R. H. Colby, *Polymer Physics* (Oxford University Press, Oxford, UK, 2003).
 - [7] J. P. Cotton, D. Decker, H. Benoit, B. Farnoux, J. Higgins, G. Jannink, R. Ober, C. Picot, and J. des Cloizeaux, *Macromolecules* **7**, 863 (1974).
 - [8] B. Farnoux, F. Boue, J. P. Cotton, M. Daoud, G. Jannink, M. Nierlich, and P. G. de Gennes, *J. Phys.* **39**, 77 (1978).
 - [9] J. C. Le Guillou and J. Zinn-Justin, *Phys. Rev. B* **21**, 3976 (1980).
 - [10] H.-P. Hsu, W. Paul and K. Binder, *Macromolecules* **43**, 3094 (2010).

- [11] H.-P. Hsu, W. Paul and K. Binder, *Europhys. Lett.* **92**, 28003 (2010).
- [12] T. Norisuye and H. Fujita, *Polymer J.* **14**, 143 (1982).
- [13] H.-P. Hsu and K. Binder, *J. Chem. Phys.* **136**, 024901 (2012).
- [14] O. Kratky and G. Porod, *J. Colloid Sci.* **4**, 35 (1949).
- [15] D. W. Schaefer, J. F. Joanny, and P. Pincus, *Macromolecules* **13**, 1280 (1980).
- [16] R. R. Netz and D. Andelman, *Phys. Rep.* **380**, 1 (2003).
- [17] H. Yamakawa and W. H. Stockmayer, *J. Chem. Phys.* **57**, 2843 (1972).
- [18] H. Yamakawa and J. Shimada, *J. Chem. Phys.* **83**, 2607 (1985).
- [19] J. Shimada and H. Yamakawa, *J. Chem. Phys.* **85**, 591 (1986).
- [20] H. Fujita, *Macromolecules* **21**, 179 (1988).
- [21] A. Tsuboi, T. Norisuye, and A. Teramoto, *Macromolecules* **29**, 3597 (1996).
- [22] H. P. Hsu, W. Paul and K. Binder, *Europhys. Lett.* **95**, 68004 (2011).
- [23] J. des Cloizeaux, *Macromolecules* **6**, 403 (1973).
- [24] G. Porod, *Z. Naturforschung* **4a**, 401 (1949).
- [25] G. Porod, *J. Polym. Sci.* **10**, 157 (1953).
- [26] A. Peterlin, *J. Polym. Sci.* **47**, 403 (1960).
- [27] W. R. Krigbaum and S. Sasaki, *J. Polym. Sci.: Polym. Phys. Ed.* **19**, 1339 (1981).
- [28] M. G. Bawendi and K. F. Freed, *J. Chem. Phys.* **83**, 2491 (1985).
- [29] M. Rawiso, R. Duplessix and C. Picot, *Macromolecules* **20**, 630 (1987).
- [30] A. L. Kholodenko, *Ann. Phys.* **202**, 186 (1990).
- [31] A. L. Kholodenko, *J. Chem. Phys.* **96**, 700 (1992).
- [32] A. L. Kholodenko, *Macromolecules* **26**, 4179 (1993).
- [33] A. J. Spakowitz and Z.-G. Wang, *Macromolecules* **37**, 5814 (2004).
- [34] S. Stepanow, *Eur. Phys. J. B* **39**, 499 (2004).
- [35] S. Stepanow, *J. Phys.: Condens. Matter* **17**, S1799 (2005).
- [36] J. S. Pedersen, M. Laso and P. Schurtenberger, *Phys. Rev. E* **54**, R5917 (1996).
- [37] J. S. Pedersen and P. Schurtenberger, *Macromolecules* **29**, 7602 (1996).
- [38] J. S. Pedersen and P. Schurtenberger, *Europhys. Lett.* **45**, 666 (1999).
- [39] D. Pötschke, P. Hickl, M. Ballauff, P.-O. Astrand, and J. S. Pedersen, *Macromol. Theory Simul.* **9**, 345 (2000).
- [40] H. Benoit, R. Duplessix, R. Ober, M. Daoud, J. P. Cotton, B. Farnoux, and G. Jannink, *Macromolecules* **8**, 451 (1975).
- [41] P. Pincus, *Macromolecules* **9**, 386 (1976).
- [42] S. B. Smith, L. Finzi, and C. Bustamante, *Science* **258**, 1122 (1992).
- [43] J. F. Marko and E. D. Siggia, *Macromolecules* **28**, 8759 (1995).
- [44] C. Pierleoni, G. Ariedi, and J.-P. Ryckaert, *Phys. Rev. Lett.* **79**, 2990 (1997).
- [45] R. R. Netz, *Macromolecules* **34**, 7522 (2001).
- [46] M.-N. Dessinges, B. Maier, Y. Zhang, M. Peliti, D. Ben-simon, and V. Croquette, *Phys. Rev. Lett.* **89**, 248102 (2002).
- [47] L. Livadaru, R. R. Netz, and H. J. Kreuzer, *Macromolecules* **36**, 3732 (2003).
- [48] T. Hugel, M. Rief, M. Seitz, H. E. Gaub, and R. R. Netz, *Phys. Rev. Lett.* **94**, 048301 (2005).
- [49] Y. Seol, G. M. Skinner, and K. Visscher, *Phys. Rev. Lett.* **93**, 118102 (2004).
- [50] A. Prasad, Y. Hori, and J. Kondev, *Phys. Rev. E* **72**, 041918 (2005).
- [51] G. Morrison, C. Hyeon, N. M. Toan, B.-Y. Ha, and D. Thirumalai, *Macromolecules* **40**, 7343 (2007).
- [52] O. A. Saleh, D. B. McIntosh, P. Pincus and N. Ribeck, *Phys. Rev. Lett.* **102**, 068301 (2009).
- [53] D. B. McIntosh, N. Ribeck and O. A. Saleh, *Phys. Rev. E* **80**, 041803 (2009).
- [54] N. M. Toan and D. Thirumalai, *Macromolecules* **43**, 4394 (2010).
- [55] A. Dittmore, D. B. McIntosh, S. Halliday, and O. A. Saleh, *Phys. Rev. Lett.* **107**, 148301 (2011).
- [56] A. Onuki, *J. Phys. Soc. Japan* **54**, 3656 (1985).
- [57] P. Lindner and R. Oberthür, *Physica B* **156 & 157**, 410 (1989).
- [58] C. Pierleoni and J.-P. Ryckaert, *Macromolecules* **28**, 5097 (1995).
- [59] T. Q. Nguyen and H.-H. Kausch (eds.) *Flexible Polymer Chains in Elongational Flow* (Springer, Berlin, 1999).
- [60] W. Reisner, K. J. Morton, R. Riehn, Y. M. Wang, Z. Yu, M. Rosen, J. C. Sturm, S. Y. Chou, E. Frey, and R. H. Austin, *Phys. Rev. Lett.* **94**, 196101 (2005).
- [61] P. Cifra, *J. Chem. Phys.* **131**, 224903 (2009).
- [62] F. Thüroff, B. Obermayer, and E. Frey, *Phys. Rev. E* **83**, 021802 (2011).
- [63] A. Yu. Grosberg and A. R. Khokhlov, *Statistical Physics of Macromolecules* (AIP Press, New York, 1994).
- [64] J. P. Wittmer, H. Meyer, J. Baschnagel, A. Johner, S. Obukhov, L. Mattioni, M. Müller and A. N. Semenov, *Phys. Rev. Lett.* **93**, 147801 (2004).
- [65] J. P. Wittmer, P. Beckrich, H. Meyer, A. Cavallo, A. Johner, and J. Baschnagel, *Phys. Rev. E* **76**, 011803 (2007).
- [66] D. Shirvanyants, S. Panyukov, Q. Liao, and M. Rubinstein, *Macromolecules* **41**, 1475 (2008).
- [67] L. Schäfer, A. Ostendorf, and J. Hager, *J. Phys. A: Math. Gen.* **32**, 7875 (1999).
- [68] H. Benoit and P. Doty, *J. Phys. Chem.* **57**, 958 (1953).
- [69] T. Neugebauer, *Ann. Phys.* **434**, 509 (1943).
- [70] H.-P. Hsu, W. Paul, and K. Binder, *J. Chem. Phys.* **129**, 204904 (2008).
- [71] S. Stepanow (private communication).
- [72] V. J. Emery and J. D. Axe, *Phys. Rev. Lett.* **40**, 1507 (1978).
- [73] A. Ricci, P. Nielaba, S. Sengupta, and K. Binder, *Phys. Rev. E* **75**, 011405 (2007).
- [74] M. Doi and s. F. Edwards, *The Theory of Polymer Dynamics* (Clarendon Press, Oxford, 1986).